AIMS Mathematics, 9(5): 11092–11121.
DOI:10.3934/math.2024544
Received: 04 January 2024
Revised: 06 February 2024
Accepted: 20 February 2024
Published: 21 March 2024

http://www.aimspress.com/journal/Math

Research article

Statistical inference of the Birnbaum-Saunders model using adaptive progressively hybrid censored data and its applications

Ahmed Elshahhat[1,*], **Refah Alotaibi**[2] **and Mazen Nassar**[3,4]

[1] Faculty of Technology and Development, Zagazig University, Zagazig 44519, Egypt

[2] Department of Mathematical Sciences, College of Science, Princess Nourah bint Abdulrahman University, P. O. Box 84428, Riyadh 11671, Saudi Arabia

[3] Department of Statistics, Faculty of Science, King Abdulaziz University, Jeddah 21589, Saudi Arabia

[4] Department of Statistics, Faculty of Commerce, Zagazig University, Egypt

* **Correspondence:** Email: aelshahhat@ftd.zu.edu.eg.

Abstract: Lately, the Birnbaum-Saunders distribution has gained a lot of attention, mainly due to its different density shapes and the non-monotonicity property of its failure rates. This work considered some estimation issues for the Birnbaum-Saunders distribution using adaptive progressive Type-II hybrid censoring. Point and interval estimations were performed employing both conventional and Bayesian methodologies. In addition to estimating the model parameters, we obtained point and interval estimates for the reliability and hazard rate functions. We looked at the method of maximum likelihood as a classical approach, and its asymptotic traits were employed to obtain approximate confidence ranges. From a Bayesian point of perspective, we considered the squared error loss function to obtain the point estimates of the various parameters. The Bayes and highest posterior density credible intervals were additionally determined. For the complex form of the posterior distribution, Bayes estimates and credible intervals were computed by sampling from the posterior distribution through the Markov chain Monte Carlo procedure. For assessing the performance of all of these estimators, a Monte Carlo simulation was employed. Several statistical standards were applied to check the effectiveness of various estimates for multiple levels of censoring with small, moderate, and large sample sizes. Finally, two scenarios for applications were given in order to highlight the usefulness of the supplied approaches.

Keywords: Birnbaum-Saunders model; adaptive progressively Type-II hybrid censoring; maximum likelihood; Bayesian estimation; Markov chain
Mathematics Subject Classification: 62F10, 62F15, 62N01, 62N02, 62N05

1. Introduction

Birnbaum and Saunders [1] proposed a two-parameter fatigue life distribution for simulating the fatigue life of metals subjected to periodic stress. They also established a natural physical rationale for the Birnbaum-Saunders (BS) model through fatigue failure produced by cyclic stress. It is also one of these distributions that was created by performing a monotone transformation on a typical normal random variable. Despite the Weibull model being the most commonly used failure time distribution, the BS population has lately attracted a lot of interest, owing to the varied forms of its density and the non-monotonicity of the nature of its failure rates. Since the work of Birnbaum and Saunders [1], extensive work has been done on this model, providing different interpretations, generalizations and inferential methods. See, for example, Ng et al. [2], Lemonte et al. [3], Pradhan and Kundu [4] and Xiuyun et al. [5]. Recently, Balakrishnan and Kundu [6] reviewed the same model in the context of various inferential approaches. Suppose Y is a random variable that follows the BS distribution, symbolized by $Y \sim \text{BS}(\boldsymbol{\Sigma})$, where $\boldsymbol{\Sigma} = (\gamma, \mu)^\top$. Define the following quantities:

$$w(y;\mu) = \sqrt{\frac{y}{\mu}} - \sqrt{\frac{\mu}{y}} \text{ and } \acute{w}(y;\mu) = \frac{1}{2\mu}\left[\sqrt{\frac{\mu}{y}} + \sqrt{\left(\frac{\mu}{y}\right)^3}\right]. \tag{1.1}$$

The probability density function (PDF) (say, $f(\cdot)$) and cumulative distribution function (CDF) (say, $F(\cdot)$) of the BS distribution can be given, respectively, as follows:

$$f(y;\boldsymbol{\Sigma}) = \frac{\acute{w}(y;\mu)}{\gamma\sqrt{2\pi}} \exp\left[-\frac{w^2(y;\mu)}{2\gamma^2}\right],\ y > 0, \tag{1.2}$$

and

$$F(y;\boldsymbol{\Sigma}) = \Phi\left[\frac{w(y;\mu)}{\gamma}\right],\ y > 0, \tag{1.3}$$

where $\Phi(\cdot)$ is the CDF of the standard normal distribution, $\gamma > 0$ is the shape parameter, and $\mu > 0$ is the scale parameter. From (1.2) and (1.3), the BS distribution's reliability function (RF) and hazard rate function (HRF) (at a mission time $t > 0$), symbolized by $R(\cdot)$ and $h(\cdot)$, are given, respectively, by

$$R(y;\boldsymbol{\Sigma}) = \Phi\left[-\frac{w(y;\mu)}{\gamma}\right],\ y > 0, \tag{1.4}$$

and

$$h(y;\boldsymbol{\Sigma}) = \frac{\acute{w}(y;\mu)\exp\left[-\frac{w^2(y;\mu)}{2\gamma^2}\right]}{\gamma\sqrt{2\pi}\Phi\left[-\frac{w(y;\mu)}{\gamma}\right]},\ y > 0. \tag{1.5}$$

Figure 1 depicts the density and failure rate shapes of the BS distribution. It exhibits that the BS density is always unimodal for all values of γ and μ. It also indicates that the shape of the HRF of the BS is an upside-down shape for all values of γ, as proved by Kundu et al. [7].

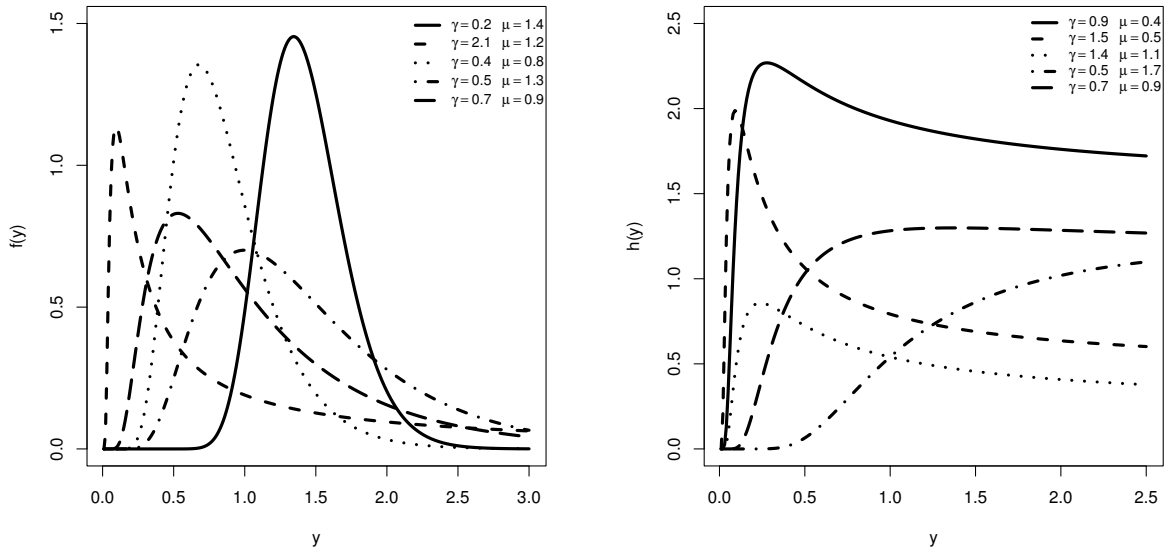

Figure 1. Density (left) and HRF (right) shapes of the BS model.

Experimenters frequently gather Type-II progressively censored (T2-PC) data in life-testing and reliability studies to decrease testing time and expenses. Balakrishnan and Aggarwala [8] presented the definition, mathematical features, and applications of the T2-PC sample. Kundu and Joarder [9] proposed a more broad censorship technique known as progressive Type-I hybrid censoring scheme. The problem with this technique is that the usable sample size is random and may turn out to be very few or zero for dependable goods. The statistical inference methods will be inefficient as a result. To deal with this shortcoming, Ng et al. [10] offered an adaptive Type-II progressive hybrid censoring (AT2-PHC) technique to improve statistical investigation efficiency. Let k, T, and $R_1, R_2, \ldots, R_k$ refer to the set amount of failures, the ideal duration on the test, and the progressive censoring plan, respectively, which are specified before beginning the examination, with the realization that the values for a particular of the R_i can vary as needed throughout the experiment. The AT2-PHC scheme can be distilled in the following manner: Consider that n components are subjected to a life test with $k < n$ then, at the time of i^{th} failure, denoted by $Y_{i:k:n}$, R_i of the remaining components are randomly removed from the test. Following this approach, we have two distinct possibilities. The first is the standard T2-PC scheme, which occurs when the time of the k^{th} failure, indicated by $Y_{k:k:n}$, comes before time T, i.e., $Y_{k:k:n} < T$. The other scenario occurs when $Y_{j:k:n} < T < Y_{j+1:k:n}$, where $(j + 1 < k)$ and $Y_{j:k:n}$ is the j^{th} failure time. In this case, we are not going to eliminate any living objects from the test by including $R_{j+1} = R_{j+2} = \cdots = R_{k-1} = 0$ and $R^* = n - k - \sum_{i=1}^{j} R_i$. This schematic makes certain that we finalize the test when we meet the required amount of failures k, and that the overall test duration does not deviate significantly from T. Let $y_{1:k:n} < \cdots < y_{j:k:n} < T < y_{j+1:k:n} < \cdots < y_{k:k:n}$ be an AT2-PHC sample from a continuous population with PDF $f(y)$ and CDF $F(y)$, with a progressive censoring plan $\mathbf{R} = (R_1, \ldots, R_j, 0, \ldots, 0, R^*)$, then, without the constant term, the likelihood function of the observed data can be presented as

$$L(\boldsymbol{\Sigma}) = \prod_{i=1}^{k} f(y_{i:k:n}) \prod_{i=1}^{j} [1 - F(y_{i:k:n})]^{R_i} [1 - F(y_{k:k:n})]^{R^*}. \tag{1.6}$$

Many studies considered the AT2-PHC scheme; see, for example, Nassar and Abo-Kasem [11], Alotaibi et al. [12], Ahmad et al. [13], Dutta et al. [14], and Elshahhat and Nassar [15], among others.

According to Balakrishnan and Kundu [6], around 200 studies explored various aspects of the BS distribution. Scarce work has been done to estimate the parameters or reliability indices of this model utilizing newly proposed censoring strategies. This may be justified due to the intricate structure of the new censoring techniques as well as the intractable formulas of the BS distribution's PDF and CDF. Therefore, we are motivated in this study to study the estimation problems of the BS distribution using the AT2-PHC scheme. This scheme is chosen because of its flexibility in ending the experiment and its ability to generalize some censoring schemes like Type-II censoring and T2-PC schemes. Moreover, the available studies consider only the estimation of the model parameters without saying anything about the estimation of the reliability indices. In order to get point and interval estimates of the shape, scale, RF, and HRF of the BS distribution, we explored two estimating approaches: maximum likelihood and Bayesian methods. First, the maximum likelihood estimates (MLEs) are obtained, followed by two approximate confidence intervals (ACIs) acquired using the normal approximation and log-transformed MLEs. For acquiring Bayesian point estimates, we address the usage of the squared error loss function and the implementation of the Markov chain Monte Carlo (MCMC) process. The Bayes credible intervals (BCIs) and highest posterior density (HPD) credible intervals are also computed. Following that, we undertake a simulation study to compare the various estimates using some statistical criteria to determine which method offers superior estimates. Two applications are addressed from a practical standpoint to demonstrate the usefulness of the proposed methodologies.

The remaining sections of the paper are formatted as follows: Section 2 discusses the MLEs and ACIs. The Bayesian estimation of the BS distribution is presented in Section 3. The discoveries of the simulation investigation are presented in Section 4. In Section 5, we present two applications to real-world data. Finally, some final thoughts are presented in Section 6.

2. Classical estimation

In this section, we will delve into the estimation of the BS distribution through the AT2-PHC scheme using the maximum likelihood approach. Employing this approach, we aim to derive both point and interval estimates of the unknown parameters as well as reliability indices. Suppose we have an AT2-PHC sample $\underline{y}$, drawn from a population that acts as the BS distribution, with progressive censoring design $\mathbf{R}$. Upon omitting the constant term, the likelihood function can then be stated by combining (1.2), (1.3), and (1.6) as follows:

$$\begin{aligned} L(\boldsymbol{\Sigma}) &= \frac{1}{\gamma^k} \exp\left\{-\frac{1}{2\gamma^2} \sum_{i=1}^{k} w^2(y_i;\mu) + \sum_{i=1}^{k} \log[\acute{w}(y_i;\mu)]\right\} \prod_{i=1}^{j} \left\{\Phi\left[-\frac{w(y_i;\mu)}{\gamma}\right]\right\}^{R_i} \\ &\times \left\{\Phi\left[-\frac{w(y_m;\mu)}{\gamma}\right]\right\}^{R^*}, \end{aligned} \tag{2.1}$$

where $w(y_i;\mu)$ and $\acute{w}(y_i;\mu)$ are as defined in (1.1). It is possible to express the log-likelihood function of (2.1) as

$$\begin{aligned}\ell(\boldsymbol{\Sigma}) &= -k\log(\gamma) - \frac{1}{2\gamma^2}\sum_{i=1}^{k} w^2(y_i;\mu) + \sum_{i=1}^{k}\log[\acute{w}(y_i;\mu)] + \sum_{i=1}^{j} R_i \log\left\{\Phi\left[-\frac{w(y_i;\mu)}{\gamma}\right]\right\} \\ &+ R^* \log\left\{\Phi\left[-\frac{w(y_m;\mu)}{\gamma}\right]\right\}. \end{aligned} \tag{2.2}$$

By differentiating the log-likelihood function in (1.2) with respect to parameters γ and μ and equating them to zero and one, we can get the MLEs of the parameters. The normal equations in this case are given by

$$\begin{aligned}\frac{\partial\ell(\boldsymbol{\Sigma})}{\partial\gamma} &= -\frac{k}{\gamma} + \frac{1}{\gamma^3}\sum_{i=1}^{k} w^2(y_i;\mu) + \frac{1}{\gamma^2}\sum_{i=1}^{j} R_i w(y_i;\mu) H[w(y_i;\mu)/\gamma] \\ &+ \frac{1}{\gamma^2} R^* w(y_m;\mu) H[w(y_m;\mu)/\gamma] = 0, \end{aligned} \tag{2.3}$$

and

$$\begin{aligned}\frac{\partial\ell(\boldsymbol{\Sigma})}{\partial\mu} &= -\frac{1}{2\gamma^2}\sum_{i=1}^{k} v(y_i;\mu) + \sum_{i=1}^{k} u(y_i;\mu) + \frac{1}{\gamma}\sum_{i=1}^{j} R_i \psi(y_i;\mu) H[w(y_m;\mu)/\gamma] \\ &+ \frac{R^*}{\gamma}\psi(y_m;\mu) H[w(y_m;\mu)/\gamma] = 0, \end{aligned} \tag{2.4}$$

where $H[y] = \phi(y)/\Phi(-y)$ and $\phi(.)$ is the PDF of the standard normal distribution,

$$v(y_i;\mu) = \frac{1}{y_i}\left[1 - \left(\frac{y_i}{\mu}\right)^2\right],\ u(y_i;\mu) = \frac{\sqrt{(\mu/y_i)^3} - \sqrt{\mu/y_i}}{4\mu^2\acute{w}(y_i;\mu)},\ \text{and}$$

$$\psi(y;\mu) = \frac{1}{2\mu}\left[\sqrt{\frac{\mu}{y_i}} + \sqrt{\frac{y_i}{\mu}}\right].$$

The simultaneous solution of (2.3) and (2.4) is the MLEs of γ and μ, denoted by $\hat{\gamma}$ and $\hat{\mu}$, respectively. To find the required MLEs, one must employ a numerical method because (2.3) and (2.4) are nonlinear equations. After obtaining the MLEs $\hat{\gamma}$ and $\hat{\mu}$, we can employ the invariance property of the MLEs to acquire the MLEs of the RF and HRF of the BS distribution as

$$\hat{R}(y;\hat{\boldsymbol{\Sigma}}) = \Phi\left[-\frac{w(y;\hat{\mu})}{\hat{\gamma}}\right],$$

and

$$\hat{h}(y;\hat{\boldsymbol{\Sigma}}) = \frac{\acute{w}(y;\hat{\mu})\exp\left[-\frac{w^2(y;\hat{\mu})}{2\hat{\gamma}^2}\right]}{\hat{\gamma}\sqrt{2\pi}\Phi\left[-\frac{w(y;\hat{\mu})}{\hat{\gamma}}\right]},$$

where $\hat{\boldsymbol{\Sigma}} = (\hat{\gamma},\hat{\mu})^\top$.

Along with obtaining the point estimates of the different parameters, it would be useful to get the interval estimates of these parameters. It is established that the MLEs' asymptotic distribution approaches normality, such that

$$\begin{pmatrix} \hat{\gamma} \\ \hat{\mu} \end{pmatrix} \approx N\left[\begin{pmatrix} \gamma \\ \mu \end{pmatrix}, \begin{pmatrix} var(\gamma) & cov(\gamma,\mu) \\ cov(\gamma,\mu) & var(\mu) \end{pmatrix}\right].$$

Here, we use the observed Fisher information matrix to estimate the variance-covariance matrix as follows:

$$\widehat{\boldsymbol{V}}(\widehat{\boldsymbol{\Sigma}}) = \begin{pmatrix} -\frac{\partial^2 \ell(\boldsymbol{\Sigma})}{\partial \gamma^2} & -\frac{\partial^2 \ell(\boldsymbol{\Sigma})}{\partial \gamma \partial \mu} \\ -\frac{\partial^2 \ell(\boldsymbol{\Sigma})}{\partial \mu \partial \gamma} & -\frac{\partial^2 \ell(\boldsymbol{\Sigma})}{\partial \mu^2} \end{pmatrix}^{-1}_{(\gamma,\mu)=(\hat{\gamma},\hat{\mu})} = \begin{pmatrix} \widehat{var}(\hat{\gamma}) & \widehat{cov}(\hat{\gamma},\hat{\mu}) \\ \widehat{cov}(\hat{\mu},\hat{\gamma}) & \widehat{var}(\hat{\mu}) \end{pmatrix}, \tag{2.5}$$

with the following elements

$$\begin{aligned} \frac{\partial^2 \ell(\boldsymbol{\Sigma})}{\partial \gamma^2} &= \frac{k}{\gamma^2} + \frac{3}{\gamma^4}\sum_{i=1}^{k} w^2(y_i;\mu) + \frac{1}{\gamma^2}\sum_{i=1}^{j} R_i w(y_i;\mu) H^{\star}[w(y_i;\mu)/\gamma] \\ &- \frac{R^*}{\gamma^2} w(y_m;\mu) H^{\star}[w(y_m;\mu)/\gamma], \end{aligned}$$

$$\begin{aligned} \frac{\partial^2 \ell(\boldsymbol{\Sigma})}{\partial \mu^2} &= -\frac{1}{2\gamma^2}\sum_{i=1}^{k} \acute{v}(y_i;\mu) + \sum_{i=1}^{k} \acute{u}(y_i;\mu) + \frac{1}{\gamma}\sum_{i=1}^{j} R_i H^{*}[w(y_m;\mu)/\gamma] \\ &+ \frac{R^*}{\gamma} H^{*}[w(y_m;\mu)/\gamma], \end{aligned}$$

and

$$\begin{aligned} \frac{\partial^2 \ell(\boldsymbol{\Sigma})}{\partial \gamma \partial \mu} &= \frac{1}{\gamma^3}\sum_{i=1}^{k} v(y_i;\mu) + \frac{1}{\gamma}\sum_{i=1}^{j} R_i \psi(y_i;\mu) H^{\circ}[w(y_m;\mu)/\gamma] \\ &+ \frac{R^*}{\gamma} \psi(y_m;\mu) H^{\circ}[w(y_m;\mu)/\gamma] = 0, \end{aligned}$$

where $w_i \equiv w(y_i;\mu)$,

$$H^{\star}[w_i/\gamma] = \frac{w_i \acute{H}[w_i/\gamma]}{\gamma^4} - \frac{2H[w_i/\gamma]}{\gamma^3},$$

$$\acute{v}(y_i;\mu) = \frac{2y_i}{\mu^3},\ \acute{u}(y_i;\mu) = \frac{2\mu y_i + y_i^2 - \mu^2}{2\mu^2(\mu + y_i)^2},$$

$$H^{*}[w_i/\gamma] = H[w_i/\gamma]\left\{\psi(y_i;\mu)\left[\acute{\psi}(y_i;\mu) - \frac{v(y_i;\mu)}{2\gamma^2} - \frac{\psi(y_i;\mu)H[w_i/\gamma]}{\gamma}\right]\right\},$$

$\acute{H}[y] = yH(y) - H^2(y)$, $\acute{\psi}(y_i;\mu) = -\frac{1}{4\mu^2}\left(\sqrt{\frac{\mu}{y_i}} + 3\sqrt{\frac{y_i}{\mu}}\right)$, and $H^{\circ}[w_i/\gamma] = \frac{w_i\acute{H}[w_i/\gamma]}{\gamma^3} - \frac{2H[w_i/\gamma]}{\gamma^2}$.

Thus, the ACIs of γ and μ can be computed, respectively, as $\hat{\gamma} \pm z_{\alpha/2}\widehat{SE}(\hat{\gamma})$ and $\hat{\mu} \pm z_{\alpha/2}\widehat{SE}(\hat{\mu})$, where $z_{\alpha/2}$ is the percentile $100(1-\alpha/2)\%$ of the standard normal distribution and $\widehat{SE}(.)$ is the standard error of estimate obtained by taking the square root of the estimated variance acquired from (2.5). Building the ACIs for RF and HR is a further important topic. The present issue is to find the variances of $\hat{R}(t)$ and $\hat{h}(t)$ given the variances of $\hat{\gamma}$ and $\hat{\mu}$. To address this issue, a particular approach is the delta method, which can be applied to approximate the required variances.

Assume that $\hat{D}_1 = (R_\gamma, R_\mu)$ and $\hat{D}_2 = (h_\gamma, h_\mu)$ are two vectors that are obtained at the MLEs $\hat{\gamma}$ and $\hat{\mu}$ and comprise the first partial derivatives of RF and HRF for γ and μ, respectively, with the following elements

$$R_\gamma = \frac{w(y;\mu)}{\gamma^2}\phi[w(y;\mu)/\gamma],\ R_\mu = \frac{\psi(y;\mu)}{\gamma}\phi[w(y;\mu)/\gamma].$$

$$h_\gamma = \frac{w(y;\mu)}{\gamma^2}\acute{H}[w(y;\mu)/\gamma] \text{ and } h_\mu = -\frac{H[w(y;\mu)/\gamma]}{\gamma}\left\{\frac{v(y;\mu)}{2\gamma} + \psi(y;\mu)H[w(y;\mu)/\gamma]\right\}.$$

The approximate estimated variances of $\hat{R}(.)$ and $\hat{h}(.)$ can be obtained as

$$\widehat{var}(\hat{R}) = (\hat{D}_1\widehat{\boldsymbol{V}}\hat{D}_1^{\top}) \text{ and } \widehat{var}(\hat{h}) = (\hat{D}_2\widehat{\boldsymbol{V}}\hat{D}_2^{\top}).$$

As a result, one can get the ACIs of RF and HRF as

$$\hat{R} \pm z_{\alpha/2}\widehat{SE}(\hat{R}) \text{ and } \hat{h} \pm z_{\alpha/2}\widehat{SE}(\hat{h}),$$

with $\widehat{SE}(\hat{R}) = \sqrt{\widehat{var}(\hat{R})}$ and $\widehat{SE}(\hat{h}) = \sqrt{\widehat{var}(\hat{h})}$. It is noteworthy to note at the end of this section that negative lower bounds may result from obtaining the ACIs using the normal approximation (ACI-NA) of the individual parameters. In such cases, one can use the normal approximation of the log-transformed (NL) MLE technique to circumvent this issue. For any parameter, say κ, the ACI using NL (ACI-NL) can be obtained as follows:

$$\hat{\kappa} \times \exp\left[\pm z_{\alpha/2}\frac{\widehat{SE}(\hat{\kappa})}{\hat{\kappa}}\right].$$

3. Bayesian estimation

We have covered point and interval parameter estimation using the frequentist approach in the last section. This section examines the Bayesian methodology under the squared error loss function. Achcar [16] started by thinking about the Bayesian inference of a BS distribution's parameters. He took into account Jeffreys prior to γ and μ to create the Bayesian inference using the complete sample. Xu and Tang [17] have taken into account the non-informative prior for the Bayesian inference of the parameters and have employed the Lindley approximation to get Bayes estimates of the unknown parameters of the BS distribution using the entire sample data. Because of the intricate formulations of the Fisher information matrix, it is difficult to establish the Jeffreys prior for the BS distribution in

the case of AT2-PHC data. Therefore, we consider the same Jeffreys prior to γ and μ as suggested by Achcar [16] as follows:

$$\pi(\mathbf{\Sigma}) \propto \frac{\zeta(\gamma^2)}{\gamma\mu}, \gamma, \mu > 0, \tag{3.1}$$

where $\zeta(\gamma^2) = \left(\frac{1}{\gamma^2} + \frac{1}{4}\right)^{0.5}$. It is to be noted that when $\zeta(\gamma^2) = 1$, the Jeffreys prior is reduced to the non-informative prior case. Combining the likelihood function in (2.1) with (3.1), one can write the joint posterior distribution over proportionality as

$$\begin{aligned} g(\mathbf{\Sigma}|\underline{\mathrm{y}}) \quad &\propto \quad \frac{\zeta(\gamma^2)}{\mu\gamma^{k+1}} \exp\left\{-\frac{1}{2\gamma^2}\sum_{i=1}^{k} w^2(y_i;\mu) + \sum_{i=1}^{k}\log[\acute{w}(y_i;\mu)]\right\} \prod_{i=1}^{j}\left\{\Phi\left[-\frac{w(y_i;\mu)}{\gamma}\right]\right\}^{R_i} \\ &\times \quad \left\{\Phi\left[-\frac{w(y_m;\mu)}{\gamma}\right]\right\}^{R^*}, \end{aligned} \tag{3.2}$$

where $\underline{\mathrm{y}}$ is the observed data. Let $\varpi(\mathbf{\Sigma})$ be any function of the parameters to be estimated, then under the squared error loss function, the Bayes estimate, denoted by $\tilde{\varpi}(\mathbf{\Sigma})$, is the posterior mean acquired as follows:

$$\tilde{\varpi}(\mathbf{\Sigma}) = \int_0^\infty \int_0^\infty \varpi(\mathbf{\Sigma}) g(\mathbf{\Sigma}|\underline{\mathrm{y}}) d\gamma d\mu. \tag{3.3}$$

The integral provided in (3.3) lacks an explicit expression. To overcome this challenge, we consider the use of the MCMC technique to create the Bayes point, BCI, and HPD estimates. The MCMC approach is used to get samples from (3.2) in order to obtain the necessary estimations. The posterior distribution is sampled using the MCMC technique, and the Bayes estimates, BCIs, and HPD intervals are then obtained using these samples. We must first obtain the full conditional distributions of the unknown parameters γ and μ in order to employ the MCMC approach. The necessary full conditional distributions of γ and μ can be obtained, respectively, from (3.2), as

$$\begin{aligned} g_\gamma(\gamma|\mu, \underline{\mathrm{y}}) \quad &\propto \quad \frac{\zeta(\gamma^2)}{\gamma^{k+1}} \exp\left\{-\frac{1}{2\gamma^2}\sum_{i=1}^{k} w^2(y_i;\mu)\right\} \prod_{i=1}^{j}\left\{\Phi\left[-\frac{w(y_i;\mu)}{\gamma}\right]\right\}^{R_i} \\ &\times \quad \left\{\Phi\left[-\frac{w(y_m;\mu)}{\gamma}\right]\right\}^{R^*}, \end{aligned} \tag{3.4}$$

and

$$\begin{aligned} g_\mu(\mu|\gamma, \underline{\mathrm{y}}) \quad &\propto \quad \frac{1}{\mu} \exp\left\{-\frac{1}{2\gamma^2}\sum_{i=1}^{k} w^2(y_i;\mu) + \sum_{i=1}^{k}\log[\acute{w}(y_i;\mu)]\right\} \prod_{i=1}^{j}\left\{\Phi\left[-\frac{w(y_i;\mu)}{\gamma}\right]\right\}^{R_i} \\ &\times \quad \left\{\Phi\left[-\frac{w(y_m;\mu)}{\gamma}\right]\right\}^{R^*}. \end{aligned} \tag{3.5}$$

Due to the complexity of the conditional distributions in (3.4) and (3.5), which cannot be reduced to any well-known distributions, we employ the Metropolis-Hastings (M-H) algorithm. For sampling

from complicated probability distributions, particularly in Bayesian estimation, the M-H algorithm is a popular MCMC technique. It is essential to Bayesian statistics because it helps approximate the posterior distribution by combining observed data and past knowledge; for more detail about the MCMC technique, see Contreras-Reyes et al. [18]. To acquire the Bayes estimates, BCIs, and HPD intervals of γ and μ, as well as the life parameters, the following processes must be followed with a normal proposal distribution (NPD) in order to obtain the necessary samples as:

Step 1. Set $l = 1$ and start with initial values $\left(\gamma^{(0)}, \mu^{(0)}\right) = (\hat{\gamma}, \hat{\mu})$.

Step 2. Simulate $\gamma^{(l)}$ from $g_\gamma(\gamma|\mu, \underline{y})$ using NPD and follow the M-H steps.

Step 3. Generate $\mu^{(l)}$ from $g_\mu(\mu|\gamma, \underline{y})$ using NPD and follow the M-H steps.

Step 4. Use $(\gamma^{(l)}, \mu^{(l)})$ to compute $R^{(k)}$ and $h^{(k)}$, respectively.

Step 5. Put $l = l + 1$.

Step 6. Repeat the process M times to generate a sequence of

$$\left[\gamma^{(l)}, \mu^{(l)}, R^{(l)}, h^{(l)}\right], l = 1, \ldots, M.$$

After discarding the first $\acute{M}$ acquired samples as a burn-in period, the Bayes estimate of any parameter, say η, can be computed as

$$\tilde{\eta} = \frac{1}{M - \acute{M}} \sum\nolimits_{l=\acute{M}+1}^{M} \eta^{(l)}.$$

In order to compute the BCI and HPD interval for η, sort the acquired sample of $\eta^{(l)}, l = \acute{M}+1, \ldots, M$ as $\eta^{(\acute{M}+1)}, \ldots, \eta^{M}$. Therefore, the $100(1-\alpha)\%$ BCI of η can be obtained as

$$\left[\eta^{(\alpha(M-\acute{M})/2)}, \eta^{((1-\alpha/2)(M-\acute{M}))}\right].$$

Moreover, the $100(1-\alpha)\%$ HPD interval of η is given by

$$\left[\eta^{(l^*)}, \eta^{\left(l^*+(1-\alpha)(M-\acute{M})/2)\right)}\right],$$

where $l^* = \acute{M} + 1, \ldots, M$ is determined such that

$$\eta^{(l^*+[(1-\alpha)(M-\acute{M})])} - \eta^{(l^*)} = \min_{1 \leqslant l \leqslant \alpha(M-\acute{M})} \left\{\eta^{(l+[(1-\alpha)(M-\acute{M})])} - \eta^{(l)}\right\},$$

where $[\varsigma]$ refers to the largest integer less than or equal to ς.

4. Monte Carlo comparisons

Monte Carlo simulations are performed in this part to test the performance of the proposed estimators of γ, μ, $R(t)$, and $h(t)$ developed in this study. From $\mathrm{BS}(\gamma, \mu) = (0.5, 1.5)$, based on various options of n (total experimental units), k (effective sample size), and T (threshold time), we simulate 1,000 AT2-PHC samples. At $t = 0.1$, the plausible values of $R(t)$ and $h(t)$ are 0.98954 and 0.12939, respectively. When $T(= 1, 2)$ and $n(40, 80)$, the number of failed subjects k is specified as a failure percentage $\frac{k}{n} \times 100\% = 50\%$ and 75%. Briefly, the next procedure reports the generation steps of the AT2-PHC strategy:

Step 1: Simulate a T2-PC sample as:

(a) Create ϑ independent observations of size k as $\vartheta_1, \vartheta_2, \ldots, \vartheta_k$.
(b) Set $\varrho_i = \vartheta_i^{\left(i+\sum_{d=k-i+1}^{k} R_d\right)^{-1}}$, $i = 1, 2, \ldots, k$.
(c) Set $u_i = 1 - \varrho_k \varrho_{k-1} \cdots \varrho_{k-i+1}$ for $i = 1, 2, \ldots, k$.
(d) Set $Y_i = F^{-1}(u_i; \gamma, \mu)$, $i = 1, 2, \ldots, k$, as the acquired T2-PC sample from BS(γ, μ).

Step 2: Find j (at $Y_j < T < Y_{j+1}$) and remove the staying items $Y_{j+2}, \ldots, Y_k$.

Step 3: From $f(y; \gamma, \mu)\left[1 - F\left(y_{j+1}; \gamma, \mu\right)\right]^{-1}$, obtain the first $k - j - 1$ order statistics with sample size $n - j - \sum_{d=1}^{j} R_d - 1$ as $Y_{j+2}, \ldots, Y_k$.

Once 1,000 AT2-PHC samples are acquired, using R programming software version 4.2.2, we utilize the following recommended packages:

- A 'maxLik' package with 'maxNR' function (by Henningsen and Toomet [19]) to implement the Newton-Raphson method in turn to evaluate the MLEs and ACIs of γ, μ, $R(t)$, and $h(t)$.
- A 'coda' package with 'run_metropolis_MCMC' function (by Plummer et al. [20]) in turn to calculate the Bayes' and credible estimates.

Following Achcar [16], we have evaluated the Bayes estimators based on both Jeffreys and non-informative priors, denoted by Pr[A] and Pr[B], respectively. Using the M-H algorithm, for γ, μ, $R(t)$, or $h(t)$, we ignore the first 2,000 of the 12,000 simulated Markovian variates as burn-in.

To examine the performance of the removal design **R**, we consider the following censoring schemes (CSs):

$$\begin{aligned}
&\text{CS-1}: \ R_1 = n - k, \quad R_i = 0 \quad \text{for} \quad i \neq 1;\\
&\text{CS-2}: R_{\frac{k}{2}} = n - k, \quad R_i = 0 \quad \text{for} \quad i \neq \frac{k}{2};\\
&\text{CS-3}: \ R_k = n - k, \quad R_i = 0 \quad \text{for} \quad i \neq k.
\end{aligned}$$

Practically, the average estimates (Av.Es) γ, μ, $R(t)$, or $h(t)$ (say ϕ) derived from the maximum likelihood (or MCMC) approach are computed by

$$\text{Av.E}\left(\breve{\phi}\right) = \frac{1}{1000}\sum_{i=1}^{1000} \breve{\phi}_{\xi}^{(i)}, \quad \xi = 1, 2, 3, 4,$$

where $\breve{\phi}^{(i)}$ is an estimate of ϕ at ith sample, $\phi_1 = \gamma$, $\phi_2 = \mu$, $\phi_3 = R(t)$, and $\phi_4 = h(t)$.

The performance of the point estimations of ϕ is evaluated based on the following two metrics:

i) Root mean squared-error (RMSE):

$$\text{RMSE}(\breve{\phi}_{\xi}) = \sqrt{\frac{1}{1000}\sum_{i=1}^{1000}\left(\breve{\phi}^{(i)} - \phi\right)^2}, \quad \xi = 1, 2, 3, 4.$$

ii) Average relative absolute bias (ARAB):

$$\text{ARAB}(\breve{\phi}_{\xi}) = \frac{1}{1000}\sum_{i=1}^{1000}\frac{1}{\phi_{\xi}}\left|\breve{\phi}_{\xi}^{(i)} - \phi_{\xi}\right|, \quad \xi = 1, 2, 3, 4.$$

The performance of the $100(1-q)\%$ interval estimations of ϕ is evaluated based on the following two metrics:

i) Average confidence length (ACL):

$$\mathrm{ACL}_{(1-q)\%}(\phi) = \frac{1}{1000}\sum_{i=1}^{1000}\left(\mathcal{U}_{\check{\phi}_{\xi}^{(i)}} - \mathcal{L}_{\check{\phi}_{\xi}^{(i)}}\right), \quad \xi = 1,2,3,4.$$

ii) Coverage percentage (CP):

$$\mathrm{CP}_{(1-q)\%}(\phi) = \frac{1}{1000}\sum_{i=1}^{1000}\mathbb{I}_{\left(\mathcal{L}_{\check{\phi}_{\xi}^{(i)}};\mathcal{U}_{\check{\phi}_{\xi}^{(i)}}\right)}(\phi), \quad \xi = 1,2,3,4,$$

respectively, where $\mathbb{I}(\cdot)$ is the indicator operator and $(\mathcal{L}(\cdot), \mathcal{U}(\cdot))$ refers to the (lower-bound, upper-bound) of an interval estimate.

In Tables 1–8, the simulated RMSE, ARAB, ACL, and CP values of γ, μ, $R(t)$, and $h(t)$ are displayed. From Tables 1–8, in regard to the smallest RMSE, ARAB, and ACL values as well as the highest CP values, we report the following comments:

- All offered estimations for the parameters and/or reliability characteristics of the BS model behaved well.
- As n(or k/n) grows, the accuracy of all estimates becomes satisfactory. The same note is also reached when the sum of removal items ($\sum_{i=1}^{k} R_i$) decreases.
- As T_i, $i = 1,2$ increase, all simulated results of γ, μ, $R(t)$, and $h(t)$ decrease. Also, when T_i, $i = 1,2$ increase, the simulated CPs grow and close to the prespecified nominal level. It is to be noted that when T increases, no additional failures are observed because the number of observed failures k is predetermined. The little improvement observed in the various criteria, like the reduction in RMSEs and ACLs when T increases, may be due to random error.
- All Bayes point estimates as well as the associated interval estimates behave better than those acquired from the likelihood approach.
- Due to the non-informative knowledge on the BS model parameters, the point and interval estimations of γ, μ, $R(t)$, or $h(t)$ developed by Pr[A] and Pr[B] are close to each other. In general, the Bayes estimates using Pr[B] perform better than those using Pr[A] in terms of minimum RMSEs, ARABs, and ACLs.
- Comparing the interval estimation methods of γ, μ, $R(t)$, or $h(t)$, it is clear that:
  - The BCI and HPD interval estimates of γ, μ, $R(t)$, or $h(t)$ are quite similar to each other.
  - The ACI-NL estimates of γ and $R(t)$ are superior to those acquired from ACI-NA estimates.
  - The ACI-NA estimates of μ and $h(t)$ are superior to those acquired from ACI-NL estimates.
  - The interval estimates of γ, μ, $R(t)$, or $h(t)$ offered using both BCI and HPD approaches are better than those acquired from ACI-NA or ACI-NL methods.
- Comparing the proposed CSs 1, 2, and 3, it is clear that:
  - The collected estimates of γ and $R(t)$ perform better via CS-3 'right-censoring' than others.
  - The collected estimates of μ and $h(t)$ perform better via CS-1 'left-censoring' than others.
- In conclusion, the Bayes' using the M-H framework is recommended for estimating the model parameters or the reliability features of the BS lifespan model.

Table 1. The Av.Es (1^{st} column), RMSEs (2^{nd} column), and ARABs (3^{rd} column) of γ.

T	n[FP%]	Scheme	MLE			MCMC-Pr[A]			MCMC-Pr[B]		
1	40[50%]	1	0.497	0.471	0.659	0.411	0.466	0.620	0.515	0.444	0.615
		2	0.477	0.435	0.623	0.421	0.423	0.587	0.517	0.414	0.549
		3	0.487	0.414	0.603	0.431	0.404	0.550	0.523	0.387	0.535
	40[75%]	1	0.497	0.331	0.593	0.422	0.311	0.518	0.518	0.302	0.485
		2	0.495	0.313	0.539	0.516	0.301	0.496	0.507	0.283	0.474
		3	0.480	0.289	0.487	0.526	0.289	0.458	0.617	0.255	0.438
	80[50%]	1	0.498	0.179	0.328	0.525	0.165	0.301	0.502	0.154	0.287
		2	0.497	0.169	0.306	0.534	0.153	0.287	0.461	0.143	0.273
		3	0.504	0.162	0.288	0.545	0.131	0.265	0.486	0.127	0.257
	80[75%]	1	0.495	0.126	0.250	0.454	0.113	0.216	0.487	0.109	0.190
		2	0.498	0.116	0.228	0.452	0.105	0.198	0.489	0.101	0.188
		3	0.456	0.105	0.207	0.457	0.099	0.175	0.472	0.093	0.168
2	40[50%]	1	0.501	0.443	0.625	0.427	0.426	0.582	0.522	0.411	0.558
		2	0.510	0.409	0.599	0.434	0.396	0.552	0.529	0.385	0.521
		3	0.581	0.386	0.564	0.431	0.378	0.518	0.523	0.366	0.507
	40[75%]	1	0.501	0.317	0.542	0.403	0.303	0.486	0.506	0.295	0.448
		2	0.518	0.291	0.477	0.427	0.282	0.456	0.515	0.269	0.426
		3	0.548	0.270	0.436	0.446	0.258	0.414	0.536	0.230	0.395
	80[50%]	1	0.503	0.171	0.320	0.509	0.153	0.279	0.486	0.146	0.262
		2	0.520	0.166	0.300	0.517	0.142	0.259	0.516	0.132	0.243
		3	0.528	0.149	0.277	0.514	0.122	0.247	0.529	0.114	0.232
	80[75%]	1	0.497	0.115	0.231	0.494	0.109	0.192	0.516	0.101	0.188
		2	0.550	0.105	0.212	0.473	0.099	0.174	0.528	0.091	0.179
		3	0.582	0.099	0.197	0.528	0.090	0.162	0.546	0.086	0.154

Table 2. The Av.Es (1^{st} column), RMSEs (2^{nd} column), and ARABs (3^{rd} column) of μ.

T	n[FP%]	Scheme	MLE			MCMC-Pr[A]			MCMC-Pr[B]		
1	40[50%]	1	1.520	0.617	0.489	1.599	0.559	0.452	1.670	0.532	0.422
		2	1.526	0.644	0.520	1.519	0.576	0.468	1.567	0.542	0.435
		3	1.520	0.692	0.534	1.537	0.627	0.484	1.571	0.587	0.452
	40[75%]	1	1.766	0.543	0.456	1.579	0.478	0.401	1.582	0.436	0.367
		2	1.575	0.586	0.478	1.569	0.517	0.417	1.672	0.492	0.391
		3	1.514	0.609	0.508	1.502	0.539	0.430	1.598	0.507	0.414
	80[50%]	1	1.599	0.454	0.354	1.720	0.429	0.341	1.728	0.382	0.340
		2	1.529	0.483	0.385	1.522	0.454	0.365	1.574	0.419	0.354
		3	1.510	0.503	0.411	1.510	0.464	0.386	1.554	0.425	0.360
	80[75%]	1	1.685	0.385	0.264	1.576	0.349	0.255	1.634	0.336	0.251
		2	1.514	0.408	0.298	1.455	0.378	0.286	1.491	0.367	0.277
		3	1.510	0.428	0.328	1.451	0.402	0.308	1.485	0.376	0.293
2	40[50%]	1	1.614	0.558	0.483	1.599	0.529	0.417	1.627	0.505	0.388
		2	1.561	0.620	0.503	1.533	0.547	0.438	1.598	0.517	0.408
		3	1.522	0.653	0.515	1.540	0.597	0.468	1.572	0.531	0.428
	40[75%]	1	1.677	0.492	0.415	1.573	0.442	0.326	1.649	0.421	0.316
		2	1.568	0.542	0.446	1.485	0.483	0.357	1.577	0.453	0.332
		3	1.518	0.601	0.474	1.493	0.514	0.389	1.597	0.486	0.377
	80[50%]	1	1.636	0.420	0.313	1.641	0.358	0.270	1.677	0.344	0.257
		2	1.545	0.437	0.345	1.487	0.377	0.292	1.565	0.361	0.284
		3	1.516	0.466	0.387	1.498	0.420	0.310	1.540	0.398	0.291
	80[75%]	1	1.680	0.329	0.259	1.592	0.294	0.201	1.497	0.282	0.193
		2	1.599	0.367	0.283	1.493	0.320	0.227	1.546	0.314	0.210
		3	1.512	0.398	0.292	1.475	0.348	0.246	1.509	0.339	0.222

Table 3. The Av.Es (1^{st} column), RMSEs (2^{nd} column), and ARABs (3^{rd} column) of $R(t)$.

T	n[FP%]	Scheme	MLE			MCMC-Pr[A]			MCMC-Pr[B]		
1	40[50%]	1	0.987	0.826	0.752	0.996	0.782	0.689	0.985	0.739	0.636
		2	0.988	0.779	0.715	0.995	0.723	0.652	0.983	0.712	0.613
		3	0.982	0.728	0.685	0.986	0.699	0.625	0.992	0.709	0.594
	40[75%]	1	0.988	0.697	0.626	0.996	0.621	0.592	0.991	0.609	0.568
		2	0.974	0.653	0.595	0.978	0.594	0.568	0.987	0.585	0.528
		3	0.967	0.613	0.573	0.984	0.541	0.546	0.982	0.522	0.517
	80[50%]	1	0.988	0.580	0.559	0.985	0.531	0.525	0.976	0.522	0.481
		2	0.989	0.533	0.525	0.978	0.513	0.491	0.972	0.496	0.469
		3	0.980	0.493	0.483	0.959	0.487	0.472	0.981	0.465	0.435
	80[75%]	1	0.989	0.448	0.428	0.993	0.415	0.387	0.989	0.408	0.365
		2	0.979	0.414	0.405	0.989	0.387	0.366	0.985	0.365	0.343
		3	0.976	0.382	0.389	0.976	0.361	0.348	0.978	0.344	0.328
2	40[50%]	1	0.986	0.788	0.716	0.992	0.726	0.637	0.989	0.709	0.611
		2	0.987	0.749	0.688	0.995	0.687	0.605	0.985	0.683	0.588
		3	0.992	0.684	0.660	0.996	0.647	0.584	0.992	0.680	0.569
	40[75%]	1	0.987	0.658	0.602	0.995	0.610	0.577	0.992	0.585	0.545
		2	0.984	0.629	0.572	0.997	0.572	0.537	0.990	0.549	0.506
		3	0.988	0.600	0.551	0.995	0.522	0.525	0.989	0.509	0.496
	80[50%]	1	0.986	0.546	0.537	0.987	0.512	0.498	0.983	0.500	0.461
		2	0.988	0.524	0.505	0.983	0.494	0.475	0.979	0.476	0.449
		3	0.992	0.472	0.465	0.992	0.467	0.449	0.986	0.446	0.424
	80[75%]	1	0.989	0.427	0.412	0.989	0.398	0.359	0.985	0.392	0.345
		2	0.987	0.395	0.389	0.991	0.371	0.338	0.988	0.351	0.329
		3	0.989	0.364	0.371	0.989	0.346	0.322	0.987	0.331	0.315

Table 4. The Av.Es (1^{st} column), RMSEs (2^{nd} column), and ARABs (3^{rd} column) of $h(t)$.

T	n[FP%]	Scheme	MLE			MCMC-Pr[A]			MCMC-Pr[B]		
1	40[50%]	1	0.129	0.528	0.767	0.135	0.447	0.742	0.129	0.428	0.713
		2	0.127	0.575	0.797	0.126	0.497	0.769	0.122	0.469	0.728
		3	0.134	0.597	0.820	0.122	0.539	0.797	0.120	0.503	0.749
	40[75%]	1	0.223	0.440	0.649	0.135	0.368	0.619	0.117	0.354	0.603
		2	0.228	0.467	0.675	0.122	0.393	0.648	0.123	0.383	0.626
		3	0.133	0.495	0.714	0.126	0.420	0.681	0.112	0.396	0.653
	80[50%]	1	0.141	0.340	0.549	0.134	0.291	0.518	0.132	0.277	0.482
		2	0.127	0.366	0.587	0.135	0.329	0.535	0.123	0.309	0.522
		3	0.131	0.386	0.617	0.130	0.351	0.585	0.120	0.329	0.566
	80[75%]	1	0.139	0.308	0.445	0.136	0.254	0.423	0.137	0.187	0.409
		2	0.129	0.312	0.477	0.127	0.268	0.447	0.142	0.233	0.421
		3	0.127	0.326	0.492	0.132	0.276	0.472	0.123	0.242	0.459
2	40[50%]	1	0.128	0.502	0.728	0.127	0.436	0.709	0.129	0.391	0.686
		2	0.133	0.526	0.756	0.124	0.477	0.735	0.131	0.450	0.694
		3	0.139	0.570	0.795	0.126	0.512	0.768	0.126	0.483	0.722
	40[75%]	1	0.126	0.420	0.610	0.123	0.357	0.597	0.121	0.345	0.585
		2	0.135	0.438	0.627	0.132	0.389	0.610	0.131	0.371	0.603
		3	0.138	0.483	0.691	0.125	0.413	0.666	0.132	0.383	0.638
	80[50%]	1	0.129	0.325	0.528	0.129	0.287	0.499	0.125	0.254	0.466
		2	0.131	0.345	0.559	0.125	0.323	0.528	0.128	0.286	0.495
		3	0.136	0.366	0.574	0.132	0.347	0.550	0.132	0.317	0.552
	80[75%]	1	0.124	0.267	0.439	0.132	0.227	0.418	0.133	0.181	0.402
		2	0.128	0.280	0.469	0.128	0.245	0.440	0.137	0.214	0.413
		3	0.130	0.311	0.488	0.129	0.263	0.465	0.126	0.224	0.435

Table 5. The ACLs (1^{st} column) and CPs (2^{nd} column) of 95% interval estimates of γ.

n[FP%]	Scheme	ACI-NA		BCI-Pr[A]		BCI-Pr[B]		ACI-NA		BCI-Pr[A]		BCI-Pr[B]	
		$T = 1$						$T = 2$					
40[50%]	1	0.437	0.926	0.415	0.928	0.399	0.930	0.428	0.929	0.402	0.931	0.396	0.933
	2	0.373	0.929	0.357	0.931	0.338	0.934	0.365	0.932	0.332	0.934	0.332	0.937
	3	0.338	0.932	0.314	0.934	0.295	0.937	0.326	0.935	0.302	0.937	0.290	0.940
40[75%]	1	0.310	0.935	0.287	0.937	0.276	0.940	0.301	0.938	0.281	0.940	0.273	0.943
	2	0.278	0.938	0.265	0.940	0.257	0.942	0.273	0.941	0.255	0.943	0.251	0.946
	3	0.256	0.940	0.246	0.942	0.236	0.945	0.252	0.943	0.242	0.945	0.231	0.948
80[50%]	1	0.236	0.942	0.224	0.945	0.219	0.948	0.234	0.945	0.216	0.948	0.211	0.951
	2	0.224	0.945	0.218	0.947	0.205	0.949	0.219	0.948	0.213	0.949	0.200	0.953
	3	0.212	0.946	0.201	0.948	0.188	0.951	0.206	0.949	0.196	0.951	0.181	0.954
80[75%]	1	0.203	0.948	0.192	0.950	0.178	0.953	0.201	0.951	0.186	0.953	0.173	0.956
	2	0.187	0.951	0.178	0.953	0.166	0.956	0.182	0.953	0.173	0.955	0.161	0.957
	3	0.172	0.952	0.169	0.954	0.160	0.957	0.170	0.955	0.165	0.957	0.157	0.959
		ACI-NL		HPD-Pr[A]		HPD-Pr[B]		ACI-NL		HPD-Pr[A]		HPD-Pr[B]	
40[50%]	1	0.426	0.928	0.409	0.929	0.393	0.932	0.422	0.930	0.397	0.932	0.389	0.934
	2	0.365	0.931	0.349	0.932	0.331	0.936	0.361	0.933	0.329	0.936	0.325	0.938
	3	0.327	0.934	0.309	0.935	0.289	0.939	0.323	0.936	0.299	0.939	0.281	0.941
40[75%]	1	0.303	0.936	0.284	0.938	0.272	0.941	0.296	0.939	0.276	0.941	0.264	0.944
	2	0.273	0.940	0.261	0.941	0.250	0.944	0.258	0.942	0.253	0.945	0.239	0.947
	3	0.216	0.941	0.240	0.943	0.231	0.946	0.209	0.944	0.235	0.947	0.224	0.949
80[50%]	1	0.232	0.943	0.221	0.946	0.214	0.949	0.225	0.946	0.213	0.949	0.205	0.952
	2	0.220	0.946	0.212	0.948	0.201	0.950	0.214	0.949	0.197	0.950	0.183	0.954
	3	0.208	0.947	0.198	0.949	0.183	0.952	0.196	0.950	0.188	0.952	0.173	0.955
80[75%]	1	0.200	0.949	0.188	0.951	0.173	0.954	0.186	0.952	0.182	0.954	0.169	0.958
	2	0.184	0.952	0.172	0.954	0.162	0.957	0.178	0.954	0.168	0.956	0.157	0.958
	3	0.169	0.953	0.163	0.955	0.155	0.958	0.164	0.956	0.159	0.959	0.152	0.960

Table 6. The ACLs (1^{st} column) and CPs (2^{nd} column) of 95% interval estimates of μ.

n[FP%]	Scheme	ACI-NA		BCI-Pr[A]		BCI-Pr[B]		ACI-NA		BCI-Pr[A]		BCI-Pr[B]	
		$T = 1$						$T = 2$					
40[50%]	1	0.608	0.935	0.585	0.936	0.573	0.938	0.584	0.935	0.574	0.937	0.566	0.940
	2	0.785	0.928	0.769	0.928	0.756	0.930	0.765	0.929	0.760	0.930	0.740	0.932
	3	0.830	0.919	0.814	0.921	0.798	0.923	0.816	0.922	0.793	0.924	0.787	0.926
40[75%]	1	0.531	0.942	0.529	0.943	0.520	0.946	0.520	0.945	0.512	0.946	0.502	0.948
	2	0.574	0.939	0.558	0.941	0.541	0.943	0.556	0.941	0.544	0.942	0.536	0.945
	3	0.588	0.936	0.579	0.938	0.569	0.940	0.572	0.938	0.561	0.941	0.559	0.942
80[50%]	1	0.418	0.954	0.410	0.955	0.389	0.957	0.415	0.954	0.402	0.957	0.381	0.958
	2	0.469	0.951	0.458	0.952	0.451	0.954	0.458	0.953	0.447	0.955	0.432	0.956
	3	0.501	0.946	0.470	0.948	0.466	0.950	0.483	0.948	0.467	0.951	0.452	0.952
80[75%]	1	0.341	0.960	0.325	0.962	0.317	0.964	0.331	0.962	0.315	0.965	0.311	0.965
	2	0.363	0.958	0.357	0.960	0.343	0.962	0.356	0.961	0.342	0.962	0.335	0.964
	3	0.408	0.956	0.385	0.958	0.374	0.959	0.404	0.957	0.373	0.960	0.368	0.961
		ACI-NL		HPD-Pr[A]		HPD-Pr[B]		ACI-NL		HPD-Pr[A]		HPD-Pr[B]	
40[50%]	1	0.613	0.933	0.595	0.935	0.582	0.937	0.604	0.934	0.580	0.936	0.571	0.939
	2	0.790	0.926	0.774	0.927	0.754	0.929	0.775	0.928	0.765	0.929	0.746	0.931
	3	0.834	0.918	0.819	0.920	0.809	0.921	0.822	0.920	0.806	0.922	0.793	0.925
40[75%]	1	0.546	0.941	0.540	0.942	0.529	0.944	0.537	0.943	0.525	0.945	0.512	0.947
	2	0.580	0.937	0.572	0.939	0.566	0.941	0.572	0.939	0.565	0.941	0.547	0.943
	3	0.594	0.935	0.583	0.937	0.574	0.938	0.590	0.936	0.578	0.939	0.562	0.941
80[50%]	1	0.429	0.952	0.416	0.953	0.409	0.955	0.419	0.953	0.408	0.956	0.394	0.958
	2	0.478	0.949	0.467	0.951	0.458	0.952	0.469	0.951	0.453	0.953	0.449	0.955
	3	0.506	0.945	0.486	0.947	0.476	0.948	0.489	0.947	0.475	0.949	0.464	0.951
80[75%]	1	0.346	0.959	0.335	0.961	0.324	0.962	0.338	0.961	0.321	0.963	0.314	0.964
	2	0.376	0.957	0.366	0.959	0.356	0.960	0.364	0.959	0.348	0.961	0.341	0.963
	3	0.412	0.954	0.392	0.956	0.385	0.958	0.409	0.956	0.385	0.958	0.379	0.960

Table 7. The ACLs (1^{st} column) and CPs (2^{nd} column) of 95% interval estimates of $R(t)$.

n[FP%]	Scheme	ACI-NA		BCI-Pr[A]		BCI-Pr[B]		ACI-NA		BCI-Pr[A]		BCI-Pr[B]	
		$T = 1$						$T = 2$					
40[50%]	1	0.628	0.922	0.598	0.925	0.585	0.928	0.614	0.924	0.586	0.926	0.578	0.929
	2	0.613	0.926	0.587	0.929	0.576	0.931	0.597	0.928	0.574	0.930	0.566	0.932
	3	0.582	0.930	0.562	0.932	0.553	0.936	0.576	0.932	0.556	0.934	0.549	0.937
40[75%]	1	0.543	0.934	0.525	0.935	0.518	0.939	0.537	0.936	0.516	0.937	0.507	0.941
	2	0.514	0.937	0.502	0.940	0.492	0.943	0.508	0.939	0.489	0.941	0.482	0.945
	3	0.497	0.939	0.483	0.942	0.476	0.944	0.486	0.941	0.478	0.943	0.460	0.945
80[50%]	1	0.457	0.943	0.449	0.944	0.425	0.947	0.437	0.945	0.427	0.946	0.416	0.949
	2	0.416	0.946	0.402	0.948	0.387	0.950	0.407	0.948	0.385	0.950	0.376	0.952
	3	0.379	0.950	0.362	0.953	0.353	0.955	0.372	0.952	0.352	0.955	0.346	0.957
80[75%]	1	0.325	0.953	0.315	0.956	0.305	0.958	0.318	0.955	0.309	0.958	0.293	0.959
	2	0.303	0.956	0.292	0.958	0.284	0.961	0.292	0.958	0.286	0.960	0.275	0.963
	3	0.285	0.958	0.276	0.960	0.259	0.963	0.280	0.960	0.269	0.962	0.251	0.964
		ACI-NL		HPD-Pr[A]		HPD-Pr[B]		ACI-NL		HPD-Pr[A]		HPD-Pr[B]	
40[50%]	1	0.616	0.924	0.590	0.926	0.579	0.930	0.604	0.925	0.577	0.928	0.566	0.931
	2	0.600	0.927	0.579	0.930	0.568	0.932	0.590	0.929	0.567	0.932	0.559	0.934
	3	0.571	0.931	0.558	0.934	0.545	0.937	0.563	0.933	0.545	0.936	0.539	0.939
40[75%]	1	0.539	0.936	0.515	0.937	0.508	0.941	0.527	0.937	0.508	0.938	0.502	0.943
	2	0.501	0.939	0.487	0.941	0.477	0.943	0.492	0.940	0.473	0.943	0.467	0.946
	3	0.487	0.941	0.476	0.943	0.465	0.945	0.482	0.942	0.469	0.945	0.453	0.947
80[50%]	1	0.437	0.945	0.425	0.945	0.412	0.949	0.423	0.946	0.413	0.947	0.409	0.950
	2	0.409	0.948	0.386	0.949	0.374	0.952	0.397	0.949	0.378	0.951	0.369	0.954
	3	0.363	0.951	0.345	0.954	0.339	0.957	0.356	0.953	0.342	0.956	0.332	0.959
80[75%]	1	0.316	0.955	0.306	0.958	0.297	0.960	0.311	0.956	0.302	0.959	0.285	0.961
	2	0.296	0.957	0.289	0.959	0.277	0.963	0.288	0.959	0.280	0.962	0.271	0.964
	3	0.276	0.959	0.270	0.961	0.250	0.964	0.270	0.961	0.266	0.963	0.244	0.965

Table 8. The ACLs (1^{st} column) and CPs (2^{nd} column) of 95% interval estimates of $h(t)$.

n[FP%]	Scheme	ACI-NA		BCI-Pr[A]		BCI-Pr[B]		ACI-NA		BCI-Pr[A]		BCI-Pr[B]	
		$T = 1$						$T = 2$					
40[50%]	1	0.315	0.948	0.299	0.951	0.282	0.953	0.308	0.950	0.288	0.953	0.279	0.955
	2	0.329	0.946	0.314	0.949	0.289	0.952	0.327	0.948	0.311	0.951	0.283	0.953
	3	0.369	0.942	0.332	0.946	0.309	0.948	0.359	0.944	0.320	0.947	0.298	0.949
40[75%]	1	0.287	0.953	0.270	0.956	0.258	0.958	0.276	0.955	0.263	0.957	0.251	0.959
	2	0.295	0.952	0.287	0.955	0.263	0.957	0.281	0.953	0.272	0.956	0.259	0.958
	3	0.305	0.950	0.291	0.953	0.278	0.955	0.302	0.951	0.281	0.955	0.272	0.957
80[50%]	1	0.234	0.961	0.227	0.964	0.219	0.965	0.228	0.963	0.218	0.965	0.214	0.966
	2	0.254	0.958	0.245	0.961	0.234	0.963	0.252	0.960	0.241	0.963	0.239	0.964
	3	0.277	0.955	0.262	0.958	0.247	0.960	0.263	0.956	0.256	0.960	0.244	0.961
80[75%]	1	0.207	0.967	0.201	0.970	0.191	0.971	0.202	0.969	0.194	0.971	0.186	0.972
	2	0.213	0.965	0.208	0.968	0.204	0.969	0.210	0.967	0.200	0.968	0.195	0.970
	3	0.227	0.963	0.216	0.966	0.210	0.968	0.218	0.965	0.207	0.967	0.202	0.969
		ACI-NL		HPD-Pr[A]		HPD-Pr[B]		ACI-NL		HPD-Pr[A]		HPD-Pr[B]	
40[50%]	1	0.367	0.931	0.349	0.933	0.339	0.936	0.359	0.933	0.326	0.935	0.331	0.937
	2	0.389	0.927	0.365	0.931	0.346	0.934	0.380	0.929	0.357	0.932	0.340	0.935
	3	0.417	0.923	0.382	0.926	0.376	0.929	0.408	0.925	0.370	0.928	0.361	0.931
40[75%]	1	0.327	0.942	0.315	0.945	0.310	0.947	0.316	0.944	0.309	0.946	0.303	0.948
	2	0.338	0.938	0.327	0.941	0.320	0.942	0.325	0.939	0.319	0.942	0.313	0.943
	3	0.354	0.934	0.341	0.935	0.331	0.938	0.348	0.936	0.329	0.937	0.324	0.940
80[50%]	1	0.274	0.948	0.258	0.951	0.246	0.953	0.261	0.949	0.246	0.952	0.238	0.955
	2	0.282	0.946	0.270	0.949	0.261	0.951	0.276	0.947	0.263	0.950	0.252	0.952
	3	0.310	0.944	0.304	0.947	0.296	0.949	0.303	0.946	0.295	0.948	0.282	0.951
80[75%]	1	0.248	0.955	0.229	0.958	0.222	0.960	0.238	0.957	0.221	0.959	0.213	0.961
	2	0.258	0.953	0.238	0.956	0.229	0.957	0.244	0.954	0.232	0.958	0.219	0.958
	3	0.261	0.950	0.246	0.953	0.237	0.955	0.255	0.952	0.241	0.954	0.229	0.956

5. Data applications

In this section, we will utilize two real datasets from the clinical and chemical sectors to demonstrate the relevance and application of the suggested approaches to real-world occurrences.

5.1. Clinical data

In this application, we shall use a clinical dataset of 56 blood samples from organ transplant recipients and assay an aliquot of each sample using a standard-recognized method of high-performance liquid chromatography. This dataset was originally given by Hawkins [21] and later rediscussed by Nassar et al. [22]. In Table 9, for computational convenience, all points of blood samples are divided by ten.

Table 9. Newly transformed blood samples.

3.50	7.10	7.70	8.70	9.30	9.90	10.4	10.9	10.9	11.2
11.8	11.8	12.5	12.7	12.9	13.0	14.8	15.1	15.3	15.6
15.9	15.9	16.2	16.6	18.5	19.8	20.3	20.6	22.1	22.7
24.1	24.4	24.5	25.4	26.6	27.1	27.5	28.0	28.5	31.8
32.7	33.6	33.9	34.0	34.6	35.0	37.0	40.2	42.8	44.0
49.8	52.1	55.6	57.8	65.3	98.0				

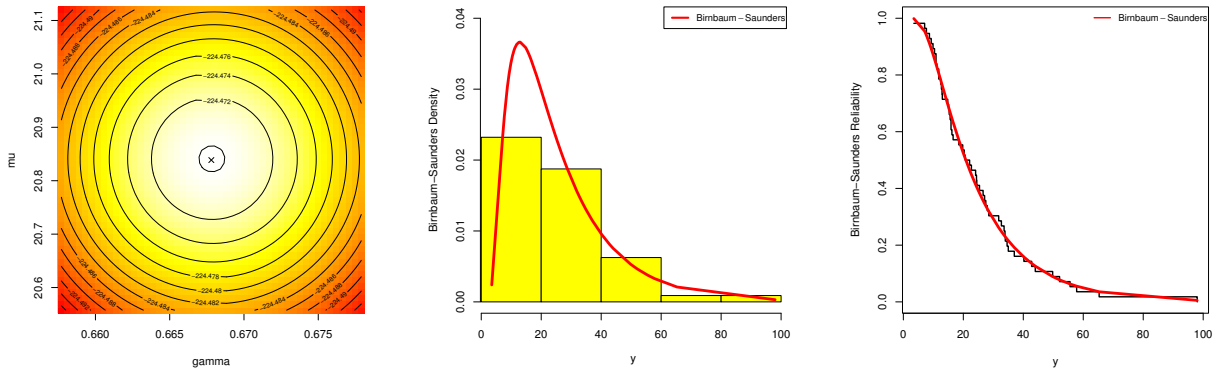

(a) Contour. (b) Density. (c) Reliability.

Figure 2. Fitting plots from blood dataset.

At first, we must determine whether the BS distribution is an acceptable model for blood data. The MLEs of γ and μ are used to estimate the Kolmogorov-Smirnov (K-S) distance and its associated P-value. The MLEs γ and μ with associated standard-errors (SEs) are 0.6678 (0.0631) and 20.839 (1.7563), respectively. At the same time, the K-S distance is 0.062 with a P-value of 0.982. This means that the BS distribution matches the blood data quite well. Also, based on the full blood dataset,

the adaptability of the BS model is highlighted via various graphical tools, namely: (a) Contour; (b) estimated density; and (c) estimated/empirical reliability; see Figure 2. Figure 2(a) shows that the MLEs $\hat{\gamma} \cong 0.6678$ and $\hat{\mu} \cong 20.839$ existed and are unique; Figure 2(b) shows that the fitted BS density line reasonably fits the histogram; and Figure 2(c) shows that the fitted BS reliability line captures the empirical reliability line adequately.

Briefly, to show the effectiveness of the BS model based on the blood dataset, the BS(γ, μ) distribution is compared with three popular models, namely: lognormal(γ, μ), Weibull(γ, μ), and gamma(γ, μ) distributions.

To establish this goal, the K-S distance (with its P-value) is obtained for each model; see Table 10. The MLEs (with their SEs) of γ and μ are also calculated and reported in Table 10. It indicates that the BS distribution is the best model compared to its competitors. It also indicates that the lognormal distribution is the next best choice among others. Figure 3 displays the histogram of the blood data and the fitted density lines, the empirical and fitted reliability functions, and the probability-probability (PP) lines. Additionally, Figure 3 supports the same fit findings.

Table 10. Summary fit of the BS, lognormal, Weibull, and gamma distributions using blood data.

Model	MLE(SE)		K-S(P-value)
	γ	μ	
BS	0.6678(0.0631)	20.841(1.7567)	0.0622(0.982)
lognormal	3.0413(0.0848)	0.6347(0.0600)	0.0711(0.939)
Weibull	1.6266(0.1578)	28.689(2.4986)	0.0918(0.733)
Gamma	2.6885(0.4798)	0.1054(0.0207)	0.1007(0.621)

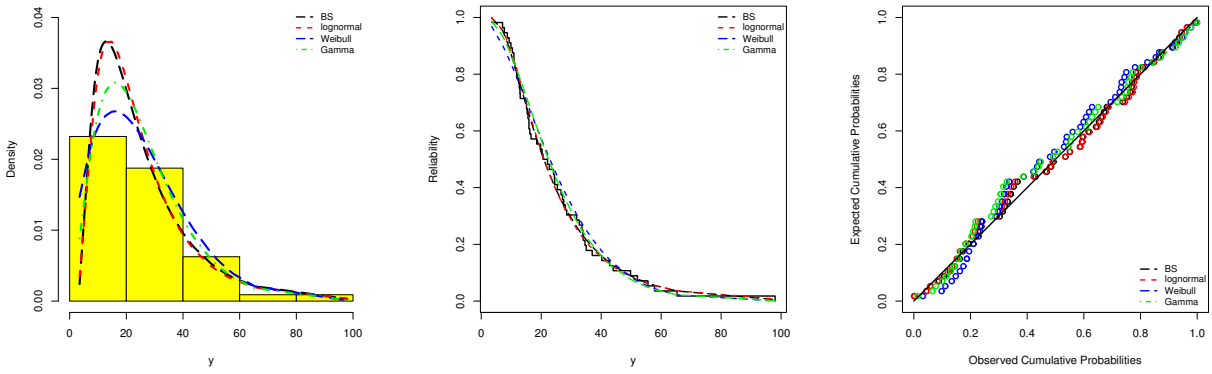

Figure 3. The density lines (left), reliability lines (center), and PP (right) of BS and its competitive models using blood data.

Using various choices of T and $\mathbf{R}$, we highlight the suggested estimates based on three AT2-PHC samples (with $k = 26$) created from the blood data; see Table 11. Using the proposed M-H steps,

we simulate 40,000 MCMC iterations and discard the first 10,000 samples as burn-in. For each S[i] for $i = 1, 2, 3$, in Table 11, the maximum likelihood and Bayes' MCMC estimates (along with their SEs) as well as 95% asymptotic (ACI-NA and ACI-NL methods) intervals and 95% credible (BCI and HPD) intervals (along with their widths) of γ, μ, $R(t)$, and $h(t)$ (at $t = 10$) are obtained; see Table 12. Both Pr[A] and Pr[B] are also utilized to obtain the MCMC estimates and associated credible interval estimates. The results in Table 12 show that the Bayes point and interval estimates of γ, μ, $R(t)$, and $h(t)$ obtained using Pr[B] perform better than other estimates in terms of minimum SEs and interval widths.

Table 11. Three AT2-PHC samples from blood data.

Sample	$T(j)$	**R**	R^*	Data
S[1]	9.5(4)	$(5^6, 0^{20})$	10	3.50, 7.10, 8.70, 9.30, 10.4, 10.9, 10.9, 11.2, 11.8, 12.7, 12.9, 13.0, 14.8, 15.1, 15.3, 15.6, 15.9, 15.9, 16.2, 16.6, 18.5, 19.8, 20.3, 20.6, 22.1, 22.7
S[2]	19.2(16)	$(0^{10}, 5^6, 0^{10})$	5	3.50, 7.10, 7.70, 8.70, 9.30, 9.90, 10.4, 10.9, 10.9, 11.2, 11.8, 11.8, 12.9, 15.3, 15.6, 15.9, 16.6, 18.5, 19.8, 20.6, 22.1, 22.7, 27.1, 27.5, 28.0, 32.7
S[3]	40.5(26)	$(0^{20}, 5^6)$	0	3.50, 7.10, 7.70, 8.70, 9.30, 9.90, 10.4, 10.9, 10.9, 11.2, 11.8, 11.8, 12.5, 12.7, 12.9, 13.0, 14.8, 15.1, 15.3, 15.6, 15.9, 27.1, 27.5, 31.8, 32.7, 40.2

Table 12. Estimates of γ, μ, $R(t)$, and $h(t)$ from blood data.

Sample	Par.	MLE		ACI-NA ACI-NL			MCMC-Pr[A] MCMC-Pr[B]		BCI BCI			HPD HPD		
		Est.	SE	lower	upper	width	Est.	SE	lower	upper	width	lower	upper	width
S[1]	γ	0.5286	0.0739	0.3837	0.6735	0.2898	0.5284	0.0193	0.4911	0.5666	0.0755	0.4906	0.5659	0.0754
				0.4019	0.6953	0.2934	0.5285	0.0099	0.5094	0.5480	0.0386	0.5093	0.5478	0.0385
	μ	17.400	1.5672	14.329	20.472	6.1433	17.401	0.0200	17.361	17.440	0.0786	17.361	17.439	0.0785
				14.585	20.760	6.1753	17.400	0.0100	17.381	17.420	0.0392	17.381	17.420	0.0392
	$R(10)$	0.8557	0.0421	0.7733	0.9382	0.1648	0.8560	0.0088	0.8389	0.8734	0.0345	0.8384	0.8729	0.0344
				0.7772	0.9423	0.1651	0.8558	0.0045	0.8470	0.8647	0.0176	0.8471	0.8647	0.0176
	$h(10)$	0.0522	0.0109	0.0308	0.0735	0.0427	0.0521	0.0008	0.0503	0.0534	0.0031	0.0505	0.0536	0.0031
				0.0346	0.0785	0.0439	0.0521	0.0004	0.0513	0.0529	0.0016	0.0513	0.0529	0.0016
S[2]	γ	0.6502	0.0933	0.4673	0.8331	0.3659	0.6502	0.0194	0.6123	0.6887	0.0764	0.6117	0.6880	0.0763
				0.4907	0.8615	0.3707	0.6502	0.0099	0.6308	0.6696	0.0388	0.6310	0.6697	0.0387
	μ	20.815	2.1698	16.562	25.067	8.5054	20.814	0.0202	20.775	20.854	0.0792	20.774	20.853	0.0791
				16.968	25.533	8.5647	20.815	0.0100	20.795	20.834	0.0393	20.795	20.835	0.0392
	$R(10)$	0.8755	0.0359	0.8052	0.9458	0.1406	0.8756	0.0071	0.8618	0.8896	0.0279	0.8614	0.8892	0.0278
				0.8080	0.9487	0.1407	0.8755	0.0036	0.8685	0.8826	0.0141	0.8685	0.8826	0.0141
	$h(10)$	0.0385	0.0075	0.0238	0.0532	0.0294	0.0385	0.0007	0.0370	0.0397	0.0028	0.0371	0.0398	0.0027
				0.0263	0.0564	0.0302	0.0385	0.0004	0.0378	0.0392	0.0014	0.0378	0.0392	0.0014
S[3]	γ	1.0767	0.1935	0.6975	1.4559	0.7584	1.0767	0.0197	1.0381	1.1158	0.0778	1.0385	1.1161	0.0776
				0.7571	1.5312	0.7742	1.0767	0.0100	1.0572	1.0962	0.0390	1.0575	1.0964	0.0389
	μ	32.257	6.4477	19.620	44.895	25.274	32.257	0.0202	32.218	32.297	0.0792	32.217	32.296	0.0792
				21.802	47.728	25.926	32.257	0.0100	32.238	32.277	0.0393	32.238	32.277	0.0392
	$R(10)$	0.8751	0.0361	0.8043	0.9459	0.1416	0.8752	0.0043	0.8666	0.8837	0.0171	0.8666	0.8837	0.0171
				0.8071	0.9489	0.1418	0.8751	0.0022	0.8709	0.8794	0.0086	0.8709	0.8794	0.0086
	$h(10)$	0.0257	0.0050	0.0158	0.0356	0.0198	0.0257	0.0003	0.0251	0.0262	0.0011	0.0251	0.0262	0.0011
				0.0175	0.0378	0.0203	0.0257	0.0001	0.0254	0.0259	0.0006	0.0254	0.0260	0.0006

Figure 4 shows the log-likelihood functions of γ and μ for all samples S[i] for $i = 1, 2, 3$, which

demonstrates that all offered frequentist estimates of γ and μ, respectively, existed and are unique. To do any more calculations based on the industrial device data in the future, we recommend using these numbers as starting points. In Table 13, using the staying 30,000 draws (from S[1] as an instance) of γ, μ, $R(t)$, and $h(t)$, several properties including mean, mode, (1^{st}, 2^{nd}, and 3^{rd}) quartiles denoted by Q_i, $i = 1, 2, 3$, standard deviation (SD) and skewness (Skew.) are reported. It supports the same facts reported in Table 12. From S[1] (as an example), to evaluate the convergence status of the staying 30,0000 MCMC iterations, trace (with Gaussian kernel) and MCMC frequencies plots γ, μ, $R(t)$, and $h(t)$ are shown in Figure 5. Other MCMC properties and plots based on S[2] and S[3] are reported in the Supplementary File.

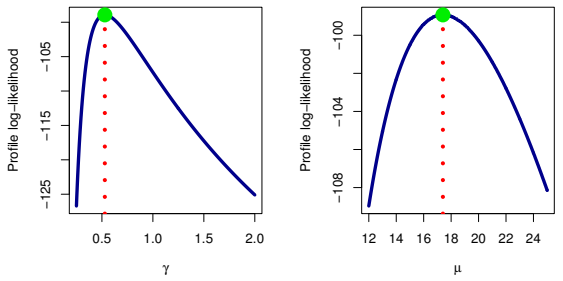

(a) S[1]

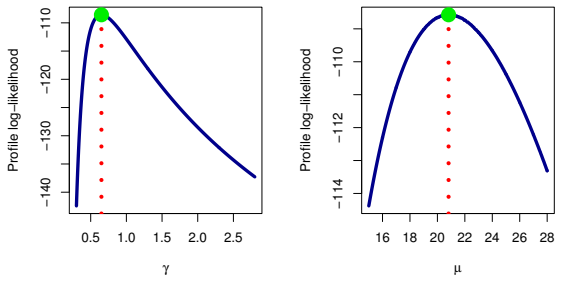

(b) S[2]

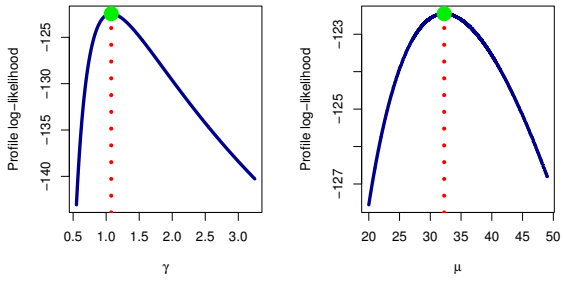

(c) S[3]

Figure 4. The log-likelihoods of γ and μ from blood data.

Table 13. Properties of γ, μ, $R(t)$, and $h(t)$ using S[1] from blood data.

Par.	MCMC-Pr[A] MCMC-Pr[B]						
	Mean	Mode	Q_1	Q_2	Q_3	SD	Skew.
γ	0.5284	0.5327	0.5152	0.5283	0.5415	0.0193	0.0208
	0.5285	0.5278	0.5219	0.5285	0.5353	0.0099	0.0191
μ	17.401	17.405	17.387	17.401	17.414	0.0200	0.0069
	17.400	17.384	17.394	17.400	17.407	0.0100	0.0125
$R(10)$	0.8560	0.8540	0.8499	0.8559	0.8619	0.0088	0.0682
	0.8558	0.8557	0.8527	0.8558	0.8588	0.0045	0.0290
$h(10)$	0.0521	0.0523	0.0516	0.0521	0.0526	0.0008	-0.5693
	0.0521	0.0522	0.0519	0.0521	0.0524	0.0004	-0.2933

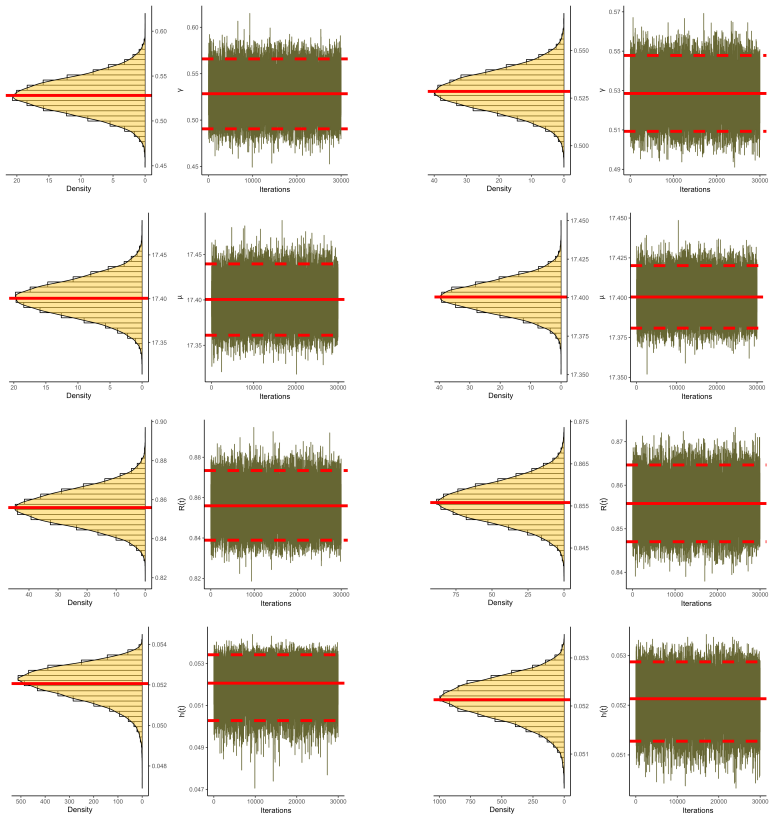

(a) MCMC-Pr[A]. (b) MCMC-Pr[B].

Figure 5. Density (left) and Trace (right) plots of γ, μ, $R(t)$, and $h(t)$ using S[1] from blood data.

The sample mean and HPD interval boundaries are displayed as solid and dotted lines in each panel,

respectively. Figure 5 indicates that the MCMC procedure converges very well and that the generated posterior estimates of γ, μ, and $R(t)$ are fairly symmetric, while those near to are being negatively skewed.

5.2. *Chemical data*

This application analyzes a chemical dataset that represents 101 observations of the fatigue life of 6061-T6 aluminum coupons cut parallel to the direction of rolling and oscillated at 18 cycles per second (with a maximum stress per cycle of 31 000 psi); see Ng et al. [23]. Table 14 lists the new converted fatigue lifetimes of the given aluminum coupons after dividing each time point by ten, for instance.

Table 14. Newly fatigued lifetimes of 6061-T6 aluminum coupons.

7.00	9.00	9.60	9.70	9.90	10.0	10.3	10.4	10.4	10.5	10.7	10.8	10.8
10.8	10.9	10.9	11.2	11.2	11.3	11.4	11.4	11.4	11.6	11.9	12.0	12.0
12.0	12.1	12.1	12.3	12.4	12.4	12.4	12.4	12.4	12.8	12.8	12.9	12.9
13.0	13.0	13.0	13.1	13.1	13.1	13.1	13.1	13.2	13.2	13.2	13.3	13.4
13.4	13.4	13.4	13.4	13.6	13.6	13.7	13.8	13.8	13.8	13.9	13.9	14.1
14.1	14.2	14.2	14.2	14.2	14.2	14.2	14.4	14.4	14.5	14.6	14.8	14.8
14.9	15.1	15.1	15.2	15.5	15.6	15.7	15.7	15.7	15.7	15.8	15.9	16.2
16.3	16.3	16.4	16.6	16.6	16.8	17.0	17.4	19.6	21.2			

From Table 14, the MLEs (SEs) of $\hat{\gamma}$ and $\hat{\mu}$ are 0.1704 (0.0120) and 13.182 (0.2226), respectively, as well as a K-S (P-value) becomes 0.0849 (0.459). Thus, the BS distribution is a reasonable model for fitting aluminum data. Again, using the complete aluminum dataset, Figure 6(a) indicates that the MLEs $\hat{\gamma} \cong 0.1704$ and $\hat{\mu} \cong 13.182$ existed and are unique; Figure 6(b)–(c) indicates that the fitted BS's density and reliability lines capture the most in the data histogram and the empirical reliability line, respectively. This fact is also supported by Figure 7.

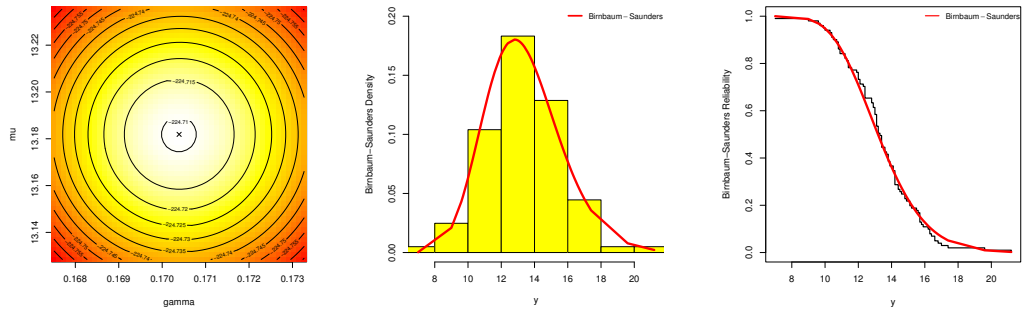

(a) Contour. (b) Density. (c) Reliability.

Figure 6. Fitting plots from aluminum dataset.

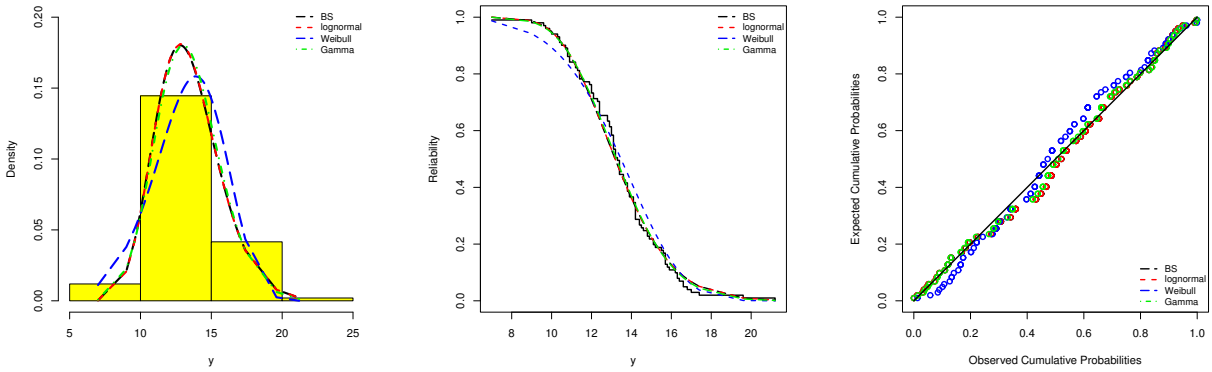

Figure 7. The density lines (left), reliability lines (center), and PP (right) of BS and its competitive models using aluminum data.

Again, based on the aluminum dataset, the BS distribution is compared to lognormal, Weibull, and gamma distributions; see Table 15. It shows that the gamma distribution is the best choice, and the BS distribution is the third-best choice among others.

Table 15. Summary fit of the BS, lognormal, Weibull, and gamma distributions using aluminum data.

Model	MLE(SE)		K-S(P-value)
	γ	μ	
BS	0.1704(0.0120)	13.182(0.2227)	0.0850(0.459)
lognormal	2.5792(0.0169)	0.1695(0.0119)	0.0838(0.477)
Weibull	6.0649(0.4226)	14.317(0.2488)	0.0990(0.275)
Gamma	35.692(4.9993)	2.6689(0.3765)	0.0727(0.660)

Using the complete aluminum data, three AT2-PHC samples (with $k = 31$) are created; see Table 16. Point and 95% interval estimates developed by maximum likelihood and Bayes' approaches of γ, μ, $R(t)$, and $h(t)$ (at $t = 10$) are obtained; see Table 17. It demonstrates that Bayes (point/interval) estimates operate similarly to frequentist estimates. The profile log-likelihood functions in Figures 8 showed that the MLEs of γ and μ existed and are unique. Based on 40,000 MCMC iterations (when the first 10,000 iterations are ignored as 'burn-in'), the acquired Bayes point and 95% BCI/HPD interval estimates are carried out using Pr[A] and Pr[B]. From Table 17, one can see that the Bayes point and interval estimates of the various parameters based on Pr[B] perform better than other estimates in terms of minimum SEs and interval widths.

Table 16. Three AT2-PHC samples from aluminum data.

Sample	$T(j)$	**R**	R^*	Data
S[1]	9.95(4)	$(7^{10}, 0^{21})$	42	7.00, 9.60, 9.70, 9.90, 10.4, 10.4, 10.5, 10.7, 10.8, 11.2, 11.3, 11.4, 11.6, 11.9, 12.0, 12.1, 12.4, 12.4, 12.8, 12.9, 13.0, 13.1, 13.2, 13.2, 13.2, 13.3, 13.4, 13.4, 13.4, 13.4, 13.4
S[2]	12.5(17)	$(0^{11}, 7^{10}, 0^{10})$	28	7.00, 9.00, 9.60, 9.70, 9.90, 10.0, 10.3, 10.4, 10.4, 10.5, 10.7, 10.8, 10.9, 11.3, 11.4, 11.9, 12.4, 12.9, 13.0, 13.4, 13.4, 13.4, 13.6, 13.6, 13.7, 13.8, 13.8, 13.9, 14.1, 14.4, 14.4
S[3]	13.9(28)	$(0^{21}, 7^{10})$	14	7.00, 9.00, 9.60, 9.70, 9.90, 10.0, 10.3, 10.4, 10.4, 10.5, 10.7, 10.8, 10.8, 10.8, 10.9, 10.9, 11.2, 11.2, 11.3, 11.4, 11.4, 11.4, 11.9, 12.0, 12.1, 12.3, 12.9, 13.7, 13.8, 14.1, 14.6

Table 17. Estimates of γ, μ, $R(t)$, and $h(t)$ from aluminum data.

Sample	Par.	MLE		ACI-NA ACI-NL			MCMC-Pr[A] MCMC-Pr[B]		BCI BCI			HPD HPD		
		Est.	SE	lower	upper	width	Est.	SE	lower	upper	width	lower	upper	width
S[1]	γ	0.2063	0.0278	0.1519	0.2606	0.1088	0.2038	0.0152	0.1755	0.2341	0.0586	0.1755	0.2341	0.0586
				0.1584	0.2685	0.1100	0.2062	0.0091	0.1885	0.2244	0.0358	0.1883	0.2241	0.0357
	μ	14.149	0.4714	13.225	15.073	1.8477	14.149	0.0201	14.110	14.189	0.0791	14.109	14.188	0.0789
				13.255	15.104	1.8490	14.149	0.0100	14.130	14.169	0.0392	14.130	14.169	0.0391
	$R(10)$	0.9546	0.0178	0.9197	0.9895	0.0698	0.9561	0.0116	0.9318	0.9766	0.0448	0.9329	0.9774	0.0445
				0.9203	0.9902	0.0698	0.9545	0.0071	0.9400	0.9679	0.0278	0.9406	0.9683	0.0277
	$h(10)$	0.0492	0.0126	0.0245	0.0739	0.0495	0.0476	0.0075	0.0327	0.0612	0.0285	0.0336	0.0619	0.0283
				0.0298	0.0814	0.0516	0.0490	0.0044	0.0400	0.0573	0.0173	0.0403	0.0575	0.0172
S[2]	γ	0.2489	0.0338	0.1826	0.3152	0.1326	0.2477	0.0159	0.2175	0.2793	0.0618	0.2178	0.2795	0.0617
				0.1907	0.3249	0.1342	0.2489	0.0093	0.2308	0.2673	0.0365	0.2310	0.2674	0.0364
	μ	14.950	0.6137	13.747	16.153	2.4056	14.950	0.0201	14.910	14.989	0.0791	14.909	14.988	0.0789
				13.794	16.203	2.4082	14.950	0.0100	14.931	14.970	0.0392	14.931	14.970	0.0391
	$R(10)$	0.9481	0.0181	0.9126	0.9835	0.0709	0.9487	0.0109	0.9264	0.9687	0.0423	0.9270	0.9691	0.0421
				0.9132	0.9842	0.0709	0.9480	0.0064	0.9351	0.9603	0.0252	0.9357	0.9608	0.0251
	$h(10)$	0.0460	0.0105	0.0254	0.0665	0.0411	0.0452	0.0054	0.0342	0.0551	0.0209	0.0349	0.0557	0.0208
				0.0294	0.0719	0.0425	0.0458	0.0031	0.0394	0.0517	0.0123	0.0396	0.0519	0.0122
S[3]	γ	0.2620	0.0378	0.1879	0.3362	0.1483	0.2609	0.0164	0.2295	0.2935	0.0639	0.2289	0.2926	0.0637
				0.1975	0.3478	0.1503	0.2620	0.0094	0.2436	0.2805	0.0369	0.2435	0.2804	0.0369
	μ	14.601	0.6420	13.343	15.859	2.517	14.601	0.0201	14.561	14.640	0.0791	14.560	14.639	0.0790
				13.395	15.915	2.5198	14.601	0.0100	14.581	14.621	0.0393	14.582	14.621	0.0392
	$R(10)$	0.9269	0.0223	0.8832	0.9706	0.0875	0.9277	0.0125	0.9026	0.9513	0.0487	0.9033	0.9518	0.0486
				0.8842	0.9717	0.0875	0.9269	0.0072	0.9126	0.9409	0.0283	0.9128	0.9410	0.0282
	$h(10)$	0.0582	0.0118	0.0350	0.0813	0.0463	0.0574	0.0050	0.0470	0.0661	0.0191	0.0477	0.0667	0.0190
				0.0391	0.0866	0.0475	0.0580	0.0028	0.0522	0.0632	0.0109	0.0525	0.0634	0.0109

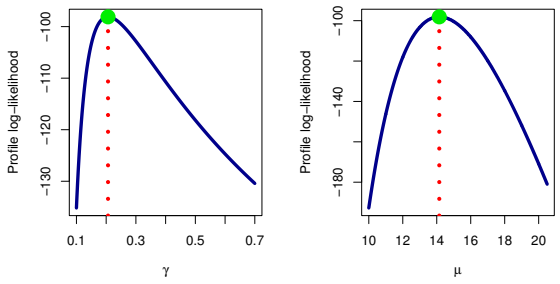

(a) S[1]

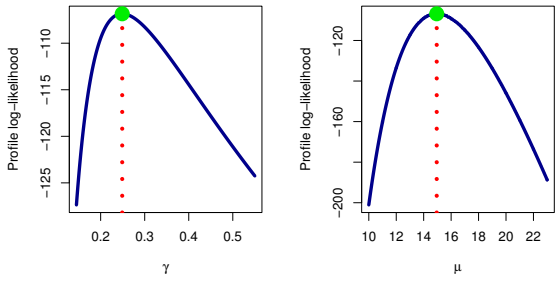

(b) S[2]

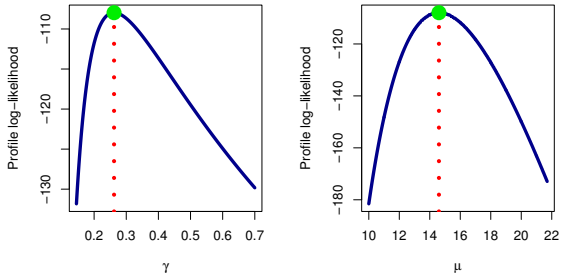

(c) S[3]

Figure 8. The log-likelihoods of γ and μ from aluminum data.

Using the remaining 30,000 MCMC variates of γ, μ, $R(t)$, and $h(t)$ for S[1] (as an example), their trace and posterior histograms are shown in Figure 9. It indicates that the simulated MCMC draws of γ, μ, $R(t)$, or $h(t)$ are mixed appropriately and behave fairly symmetrically. Again, using S[1], the same properties reported in Table 13 are recomputed and provided in Table 18. All findings reported in Table 18 support the same facts listed in Table 17. As supplementary materials, the same plots (in Figure 9) and the same properties (in Table 18) of γ, μ, $R(t)$, and $h(t)$ based on S[2] and S[3] are presented.

Finally, the findings of the study based on two real-world datasets from the clinical or chemical fields revealed that the suggested BS model is useful in highlighting the relevance of the supplied estimating approaches to real-world occurrences. In a similar way, one can easily perform our

computational design for any other dataset from other sectors, such as physics, environment, business and fishery.

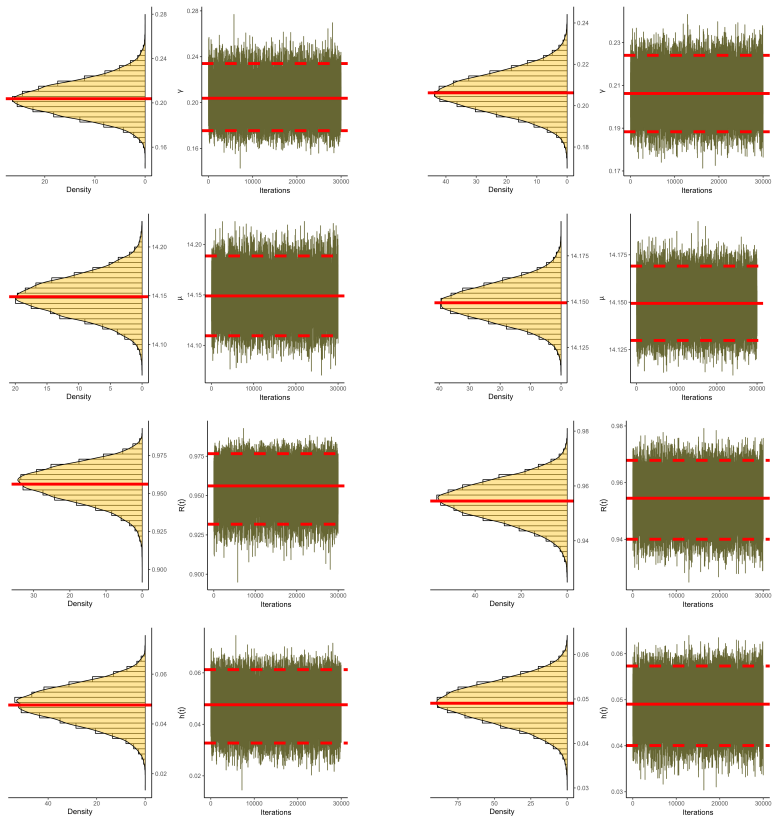

(a) MCMC-Pr[A]. (b) MCMC-Pr[B].

Figure 9. Density (left) and Trace (right) plots of γ, μ, $R(t)$, and $h(t)$ using S[1] from aluminum data.

Table 18. Properties of γ, μ, $R(t)$, and $h(t)$ using S[1] from aluminum data.

Par.	MCMC-Pr[A] MCMC-Pr[B]						
	Mean	Mode	Q_1	Q_2	Q_3	SD	Skew.
γ	0.2038	0.1930	0.1935	0.2033	0.2139	0.0150	0.1452
	0.2062	0.2131	0.2000	0.2061	0.2124	0.0091	0.0406
μ	14.149	14.110	14.135	14.149	14.163	0.0201	0.0207
	14.149	14.136	14.143	14.149	14.156	0.0100	0.0156
$R(10)$	0.9561	0.9617	0.9486	0.9569	0.9643	0.0115	-0.3400
	0.9545	0.9487	0.9498	0.9547	0.9594	0.0071	-0.1534
$h(10)$	0.0476	0.0436	0.0427	0.0478	0.0528	0.0073	-0.1625
	0.0490	0.0528	0.0461	0.0492	0.0521	0.0044	-0.1625

6. Concluding remarks

We checked the estimations of the BS distribution, including its unknown parameters, RF, and HRF, in the context of adaptive progressively Type-II hybrid censored data. To obtain the MLEs, numerical techniques must be used to solve the normal equations. Two approximate confidence intervals are considered using the asymptotic properties of MLEs. The delta approach is used to approximate the variances of the estimators of the RF and HRF. The MCMC approach has been applied to determine the Bayes estimates for the BS distribution based on the squared error loss function. In addition, the Bayes and highest posterior density credible intervals are considered. We undertake a simulation analysis that takes into account different sample sizes and censoring schemes to evaluate both point estimation approaches and four interval estimations. A lot of conclusions can be drawn from the simulation study's findings, which support the superiority of Bayes estimates over conventional estimates. At last, two real-world datasets were explored to highlight how various suggested approaches could potentially be used in daily life. As a future work, using the proposed censored sample, one can easily expand the proposed maximum likelihood calculations by performing the expectation-maximization algorithm of the BS distribution.

Use of AI tools declaration

The authors declare they have not used Artificial Intelligence (AI) tools in the creation of this article.

Acknowledgments

This research was funded by Princess Nourah bint Abdulrahman University Researchers Supporting Project number (PNURSP2024R50), Princess Nourah bint Abdulrahman University, Riyadh, Saudi Arabia.

The authors would desire to express their thanks to the editor and the four anonymous referees for useful suggestions and valuable comments.

Conflict of interest

The authors declare that they have no conflicts of interest.

References

1. Z. W. Birnbaum, S. C. Saunders, A probabilistic interpretation of Miner's rule, *SIAM J. Appl. Math.*, **16** (1968), 637–652. https://doi.org/10.1137/0116052
2. H. K. T. Ng, D. Kundu, N. Balakrishnan, Point and interval estimation for the two-parameter Birnbaum-Saunders distribution based on Type-II censored samples, *Comput. Stat. Data An.*, **50** (2006), 3222–3242. https://doi.org/10.1016/j.csda.2005.06.002
3. A. J. Lemonte, F. Cribari-Neto, K. L. P. Vasconcellos, Improved statistical inference for the two-parameter Birnbaum-Saunders distribution, *Comput. Stat. Data An.*, **51** (2007), 4656–4681. https://doi.org/10.1016/j.csda.2006.08.016

4. B. Pradhan, D. Kundu, Inference and optimal censoring schemes for progressively censored Birnbaum-Saunders distribution, *J. Stat. Plan. Infer.*, **143** (2013), 1098–1108. https://doi.org/10.1016/j.jspi.2012.11.007

5. X. Y. Peng, Y. Xiao, Z. Z. Yan, Reliability analysis of Birnbaum-Saunders model based on progressive type-II censoring, *J. Stat. Comput. Sim.*, **89** (2019), 461–477. https://doi.org/10.1080/00949655.2018.1555251

6. N. Balakrishnan, D. Kundu, Birnbaum-Saunders distribution: A review of models, analysis, and applications, *Appl. Stoch. Model. Bus.*, **35** (2019), 4–49. https://doi.org/10.1002/asmb.2348

7. D. Kundu, N. Kannan, N. Balakrishnan, On the hazard function of Birnbaum-Saunders distribution and associated inference, *Comput. Stat. Data An.*, **52** (2008), 2692–2702. https://doi.org/10.1016/j.csda.2007.09.021

8. N. Balakrishnan, R. Aggarwala, *Progressive censoring: theory, methods, and application*, Boston: Birkhäuser, 2000. https://doi.org/10.1007/978-1-4612-1334-5

9. D. Kundu, A. Joarder, Analysis of Type-II progressively hybrid censored data, *Comput. Stat. Data An.*, **50** (2006), 2509–2528. https://doi.org/10.1016/j.csda.2005.05.002

10. H. K. T. Ng, D. Kundu, P. S. Chan, Statistical analysis of exponential lifetimes under an adaptive Type-II progressive censoring scheme, *Nav. Res. Log.*, **56** (2009), 687–698. https://doi.org/10.1002/nav.20371

11. M. Nassar, O. E. Abo-Kasem, Estimation of the inverse Weibull parameters under adaptive type-II progressive hybrid censoring scheme, *J. Comput. Appl. Math.*, **315** (2017), 228–239. https://doi.org/10.1016/j.cam.2016.11.012

12. R. Alotaibi, A. Elshahhat, H. Rezk, M. Nassar, Inferences for Alpha power exponential distribution using adaptive progressively type-II hybrid censored data with applications, *Symmetry*, **14** (2022), 651. https://doi.org/10.3390/sym14040651

13. H. H. Ahmad, M. M. Salah, M. S. Eliwa, Z. A. Alhussain, E. M. Almetwally, E. A. Ahmed, Bayesian and non-Bayesian inference under adaptive type-II progressive censored sample with exponentiated power Lindley distribution, *J. Appl. Stat.*, **49** (2022), 2981–3001. https://doi.org/10.1080/02664763.2021.1931819

14. S. Dutta, S. Dey, S. Kayal, Bayesian survival analysis of logistic exponential distribution for adaptive progressive Type-II censored data, *Comput. Stat.*, **2023** (2023), 1–47. https://doi.org/10.1007/s00180-023-01376-y

15. A. Elshahhat, M. Nassar, Analysis of adaptive Type-II progressively hybrid censoring with binomial removals, *J. Stat. Comput. Sim.*, **93** (2023), 1077–1103. https://doi.org/10.1080/00949655.2022.2127149

16. J. A. Achcar, Inferences for the Birnbaum-Saunders fatigue life model using Bayesian methods, *Comput. Stat. Data An.*, **15** (1993), 367–380. https://doi.org/10.1016/0167-9473(93)90170-X

17. A. C. Xu, Y. C. Tang, Reference analysis for Birnbaum-Saunders distribution, *Comput. Stat. Data An.*, **54** (2010), 185–192. https://doi.org/10.1016/j.csda.2009.08.004

18. J. E. Contreras-Reyes, F. O. L. Quintero, R. Wiff, Bayesian modeling of individual growth variability using back-calculation: Application to pink cusk-eel (Genypterus blacodes) off Chile, *Ecol. Model.*, **385** (2018), 145–153. https://doi.org/10.1016/j.ecolmodel.2018.07.002

19. A. Henningsen, O. Toomet, maxLik: A package for maximum likelihood estimation in R, *Comput. Stat.*, **26** (2011), 443–458. https://doi.org/10.1007/s00180-010-0217-1

20. M. Plummer, N. Best, K. Cowles, K. Vines, Coda: Convergence diagnosis and output analysis for MCMC, *R. News*, **6** (2006), 7–11.

21. D. M. Hawkins, Diagnostics for conformity of paired quantitative measurements, *Stat. Med.*, **21** (2002), 1913–1935. https://doi.org/10.1002/sim.1013

22. M. Nassar, R. Alotaibi, A. Elshahhat, Complexity analysis of E-Bayesian estimation under type-II censoring with application to organ transplant blood data, *Symmetry*, **14** (2022), 1308. https://doi.org/10.3390/sym14071308

23. H. K. T. Ng, D. Kundu, N. Balakrishnan, Modified moment estimation for the two-parameter Birnbaum-Saunders distribution, *Comput. Stat. Data An.*, **43** (2003), 283–298. https://doi.org/10.1016/S0167-9473(02)00254-2

AIMS Press